JOC The Journal of Organic Chemistry

Article

Syntheses of Diverse Donor-Substituted Bisbenzofuro[2,3-b:3',2'-e]pyridines (BBZFPys) via Pd Catalysis, and Their Photophysical Properties

Yuhei Itai, Yuji Nishii, Patrycja Stachelek, Przemyslaw Data, Youhei Takeda, Satoshi Minakata, and Masahiro Miura

J. Org. Chem., **Just Accepted Manuscript** • DOI: 10.1021/acs.joc.8b01451 • Publication Date (Web): 13 Aug 2018

ACS Publications

is published by the American Chemical Society. 1155 Sixteenth Street N.W., Washington, DC 20036

Syntheses of Diverse Donor-Substituted Bisbenzofuro[2,3-*b*:3',2'-*e*]pyridines (BBZFPys) via Pd Catalysis, and Their Photophysical Properties

Yuhei Itai,[†] Yuji Nishii,[†,‡] Patrycja Stachelek,[§] Przemyslaw Data,*[,§,∥,⊥] Youhei Takeda,*[,†] Satoshi Minakata,[†] and Masahiro Miura*[,†]

[†]*Department of Applied Chemistry, Graduate School of Engineering, Osaka University, Yamadaoka 2-1, Suita, Osaka 565-0871, Japan*

[‡]*Frontier Research Base for Global Young Researchers, Graduate School of Engineering, Osaka University, Yamadaoka 2-1, Suita, Osaka 565-0871, Japan*

[§]*Durham University, Physics Department, South Road, Durham DH1 3LE, United Kingdom*

[∥]*Faculty of Chemistry, Silesian University of Technology, M. Strzody 9, 44-100 Gliwice, Poland*

[⊥]*Center of Polymer and Carbon Materials, Polish Academy of Sciences, M. Curie-Sklodowskiej 34, 41-819 Zabrze, Poland*

przemyslaw.data@durham.ac.uk; takeda@chem.eng.osaka-u.ac.jp; miura@chem.eng.osaka-u.ac.jp

Table of Contents

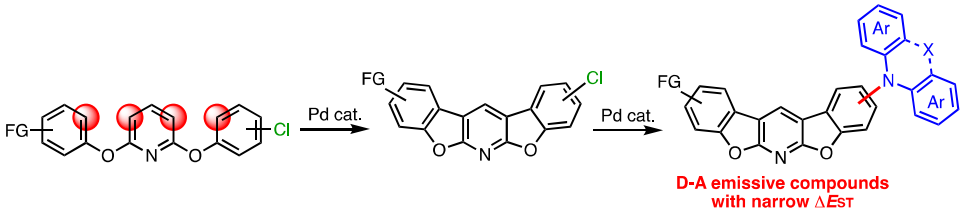

Abstract

A series of bisbenzofuro[2,3-*b*:3',2'-*e*]pyridines (BBZFPys) bearing a chlorine functionality have been efficiently synthesized through a Pd-catalyzed double oxidative intramolecular C–H/C–H coupling of mono-chlorinated 2,6-diaryloxypyridines. The subsequent Buchwald-Hartwig amination of the chlorinated BBZFPys allowed for the access to a new class of donor-acceptor (D-A) π-conjugated compounds that comprise of BBZFPy as an electron-acceptor (A) and diarylamines as a donor (D) units. The investigation of the steady-state photophysical properties of the prepared D-A compounds revealed that they are emissive in both of solution and solid states in blue-to-green color region. The singlet-triplet energy splitting (ΔE_{ST}) was found much smaller than that of substituent-free BBZFPy (0.70 eV), ranging from 0.01 to 0.56 eV. The time-resolved spectroscopy revealed that the D-A compounds comprising of a bis(*tert*-butyl)carbazole as the D and CF_3-attached BBZFPy as the A showed delayed fluorescence

(DF) in non-polar matrix host material (Zeonex®), while in a polar matrix (DPEPO), room-temperature phosphorescence (RTP) was faintly observed. Furthermore, organic light-emitting diodes (OLEDs) fabricated with the D-A compounds as a blue-emitter showed a moderate external quantum efficiencies (EQEs) up to 1.5%.

Introduction

Benzofuro[2,3-*b*]pyridines (BZFPys) constitute an important scaffold in medicinal chemistry and materials science. For example, 4-amino or aryl-substituted BZFPys serve as a class of multi-kinase inhibitors,[1] while BZFPys having an electron-donating group at the 6-position serve as promising bipolar host materials for blue phosphorescent organic light-emitting diodes (PHOLEDs).[2] Traditionally, BZFPYs are prepared through intramolecular S_NAr cyclization of the diazonium salts derived from 3-amino-2-phenoxypyridines. Nevertheless, this method requires the preparation of explosive diazonium compounds, and the product yields are typically low.[1] Recent progress mainly focuses on the utilization of transition-metal catalysis, allowing milder reaction conditions. Ames and Opalko reported a Pd-catalyzed Heck-type cyclization of 2-(2-bromophenoxy)pyridine to give non-substituted BZFPy, albeit in a low yield,[3a] while the Li group developed a Pd-catalyzed high-yielding protocol that comprises of the stannylation of 3-iodo-2-(2-iodophenoxy)pyridine and the subsequent intramolecular Stille cross-coupling.[3b] Another efficient route to BZFPys involves a CuTC-mediated intramolecular Ullmann-type *O*-cyclization of 2-(2-chloropyridin-3-yl)phenols.[3c] A Rh-catalyzed CN-cleaving cyclization of 2-(2-chlorophenoxy)nicotinonitrile developed by the Tobisu and Chatani group constitutes an intriguing route to BZFPy skeleton.[3d] Nevertheless, these precedent methods use the pre-functionalized aryloxypyridine substrates, and therefore, multi steps are required from readily available organic compounds.

Oxidative C–H/C–H coupling of heteroatom-linked polyarenes would be one of the most atom-economical, straightforward, and diverse approaches to polycondensed heteroacenes, because a large variety of the diaryl ethers, amines, and sulfides are readily available.[4–6] As a program of our research on direct C–H functionalization of aromatic compounds via transition-metal catalysis,[7] we have contributed to the development of highly atom- and step-economical synthetic methods for ladder-type heteroacenes (e.g., thienobenzofurans[5a] and benzobis- and benzotrisbenzofurans).[5b] More recently, we have developed a Pd-catalyzed oxidative intramolecular double C–H/C–H coupling of 2,6-diaryloxypyridines to give bisbenzofuro[2,3-*b*:3',2'-*e*]pyridines (BBZFPys) (Eq. 1).[6] The preliminary investigation of the physicochemical properties of substituent-free BBZFPy revealed that its chloroform solution emits a violet fluorescence (λ_{em} 360 nm) with a narrow Stokes shift ($\Delta\lambda$ 1041 cm^{-1}) and a high photoluminescence quantum yield (PLQY) (Φ_F 0.70). Other

interesting physicochemical aspects involve a wide HOMO/LUMO gap (E_g 3.44 eV), a high triplet energy (E_T 2.88 eV), and a high electron affinity (EA: 2.67 eV),[6] indicating that the BBZFPy can serve as a unique electron accepting building block for organic functional materials.

Donor-acceptor (D-A) π-conjugated organic compounds have increasingly emerged as useful scaffolds for organic functional materials such as organic photovoltaics (OPVs),[8a] organic light-emitting diodes (OLEDs),[8b] and bio-imaging probes.[8c] Specifically, twisted D–A π-conjugated compounds that show charge transfer (CT) emissions have rapidly attracted much attention as promising thermally activated delayed fluorescence (TADF) materials over the last several years.[8b,9] To gain efficient TADF with D-A conjugated systems, the reverse intersystem crossing (RISC) from the triplet excited state (T_1) to the singlet charge transfer state (^{1}CT) should be promoted by modifying the D/A combinations and the D–A dihedral angles.[10] As one of the key criteria for designing TADF-active molecules, it is desirable to tune the singlet-triplet energy splitting (ΔE_{ST}) to be almost zero.

Based on these backgrounds, we decided to expand our oxidative intramolecular C–H/C–H coupling method[6] to the preparation of diverse D-A-type BBZFPys and to investigate the photophysical properties of the resulting D-A compounds with the aim at applying to organic emitters in OLED devices. Herein we disclose a highly atom- and step-economical synthetic strategy for the preparation of D-A-type BBZFPys through a sequential protocol comprising of a Pd-catalyze intramolecular C–H/C–H oxidative coupling of monochloro 2,6-diaryloxypyridines and the subsequent Buchwald-Hartwig amination (Eq. 2). Photophysical properties of the D-A compounds in solution and solid states also have been investigated. Furthermore, applications of the D-A compounds as a blue emitter in OLED devices have been demonstrated.

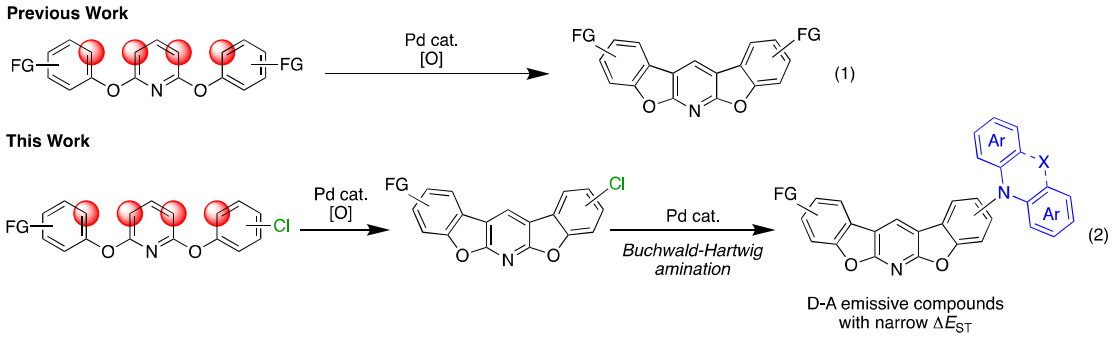

Results and Discussion

Design and Syntheses

As an initial study, theoretical calculation of a D-A type BBZFPy in the gas phase was conducted by the DFT method at the B3LYP/6-31G level (Figure 1; for the details, see the Supporting Information). The optimized structure of the D-A compound in the ground state takes

the twisted conformation around the C–N bond with the dihedral angle being 58.5 ° (Figure 1), which would be the consequence of the balance between the steric repulsion of aromatic C–H groups of the D and A units and weak π-system conjugation. This propensity of the D-A twisted structure was rationalized by the potential energy surface (PES) scan of the grond state of this D-A compound around the D-A dihedral angle (Figure S1). The ΔE_{ST} of the simplest D-A BBZFPy compound was estimated by the time-dependent DFT (TDDFT) method at the same level using the optimized structure of the ground state (for the details, see the Supporting Information). Although the TDDFT calculation using the B3LYP functional often gives substantial errors for the charge transfer excited states of D-A type molecules, it is still useful for a brief estimation of ΔE_{ST} of designed molecules, due to the low calculation cost. Owing to the twisted structure, the HOMO and LUMO are distinctly separated (Figure 1), and thereby ΔE_{ST} being substantially reduced to 0.26 eV, which is much narrower than that of BBZFPy (0.70 eV).[6]

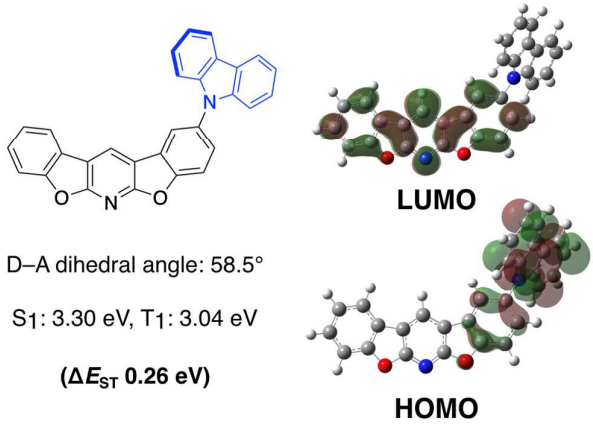

Figure 1. The illustrative summary of the theoretical calculation by the DFT method.

As starting substrates, unsymmetric 2,6-diaryloxypyridines **2** were readily prepared by the sequential double substitution of the dihalo groups of 2,6-dichloro- and dibromopyridines with phenol derivatives (Scheme 1). The treatment of dichloropyridines with about a half equivalent of phenol derivatives under basic conditions (*Conditions A*, Scheme 1) selectively gave mono-substituted products **1a**–**1d** in high yields (88–93% based on the amount of phenol substrates), while in the case of dibromopyridine, Cu-catalyzed Ullmann-type *O*-arylation[11] gave the corresponding monoaryloxy bromopyridine **1e** and **1f** in moderate yields (*Conditions B*, Scheme 1). Using similar reaction conditions (*Conditions C* and *D*, Scheme 1),[12] the remaining halogen group was substituted with phenol derivatives to give a variety of unsymmetric diaryloxypyridines **2**.

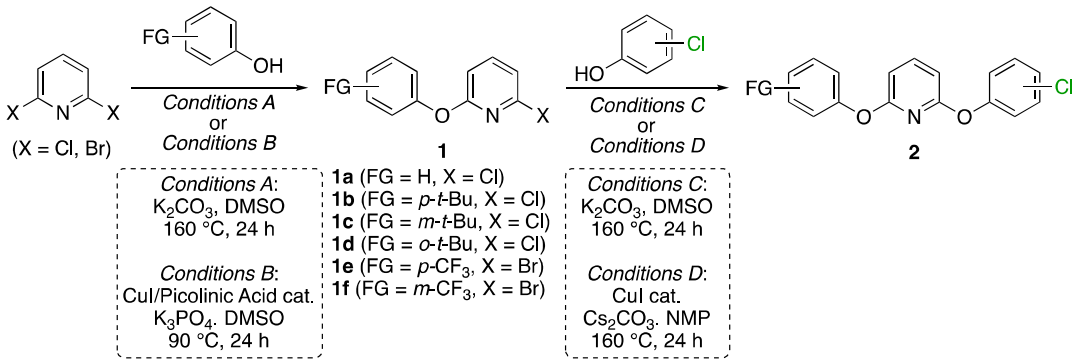

Scheme 1. Preparation of unsymmetric chloro-bearing 2,6-diaryloxypyridines **2**.

To synthesize precursors for D-A-type BBZFPys and to verify the generality of the previously developed oxidative C–H/C–H coupling, diaryloxypyridines **2** were subjected to the slightly modified coupling reaction conditions (Table 1).[6] In the presence of $Pd(TFA)_2$ as a catalyst and AgOAc as a stoichiometric oxidant, *p*-chlorinated diphenoxypyridine **2a** smoothly underwent the double C–H/C–H coupling to give monochlorinated BBZFPy product **3a** in a good yield (80%). The oxidative reactions using diaryloxypyridines that have a *para*-*tert*-butyl group on a benzene ring and a *p*- and *m*-Cl substituent on the other aryl moiety (**2b** and **2c**) gave **3b** and **3d**, respectively, in good yields. On the other hand, the reactions of pyridines with *meta*-*tert*-butyl and *p*-Cl (**2d**) and *m*-Cl (**2e**) functionalities afforded the corresponding products **3d** and **3e** in low yields. From the diaryloxypyridines with an *ortho*-*tert*-butyl substituent (**2f** and **2g**), cyclized products **3f** and **3g**, respectively, in moderate yields (63% and 68%). To enhance the electron-accepting ability of the BBZFPy core, CF_3-incorporated substrates **2h** and **2i** were subjected to the reaction conditions to afford electron-deficient BBZFPys **3h** and **3i**, respectively, in moderate yields. Under these oxidative conditions, the chloro functionality of BBZFPy remains intact, which would be a merit of using this atom- and step-economical synthetic method.

Table 1. Scope of the Pd-catalyzed intramolecular double C–H/C–H oxidative coupling of **2**[a]

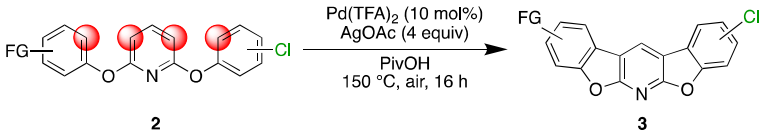

Substrate	Product (Isolated yield)
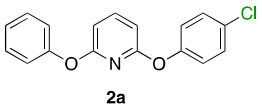 **2a**	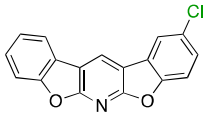 **3a** (80%)[b]
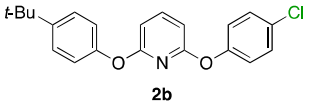 **2b**	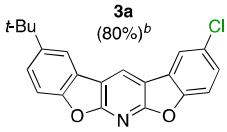 **3b** (75%)
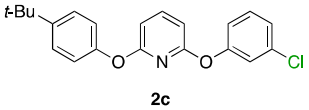 **2c**	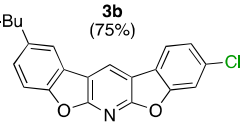 **3c** (75%)
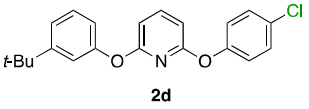 **2d**	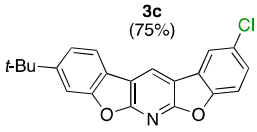 **3d** (19%)
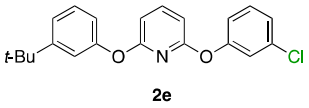 **2e**	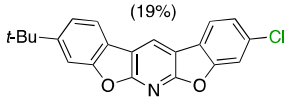 **3e** (7%)
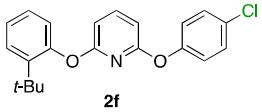 **2f**	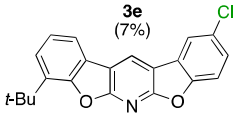 **3f** (63%)
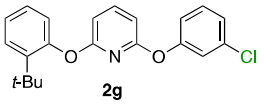 **2g**	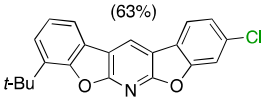 **3g** (68%)
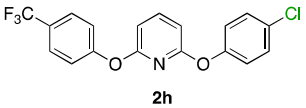 **2h**	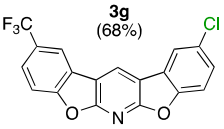 **3h** (69%)
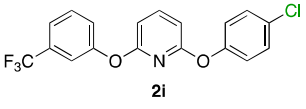 **2i**	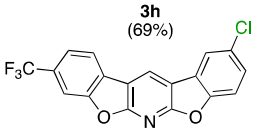 **3i** (46%)

[a]Reaction conditions: **2** (0.40 mmol), $Pd(TFA)_2$ (40 μmol, 10 mol%), and AgOAc (1.60 mmol, 4.0 equiv) in PivOH (4.0 mL) in a 10 mL Schlenk tube at 150 °C for 16 h under air. [b]**2a** (0.40 mmol), $Pd(TFA)_2$ (80 μmol, 20 mol%), and AgOAc (6.0 equiv) in PivOH (4.0 mL) in a 10 mL Schlenk tube at 150 °C for 16 h under air.

With a variety of BBZFPy building blocks in hand, a series of diarylamines were incorporated into the acceptor core through the Pd-catalyzed Buchwald-Hartwig amination (Table 2). MoPhos was found effective for executing the challenging C–Cl amination.[13] The amination of the simplest BBZFPy **3a** with carbazole and carbazolylcarbazole gave **4aa** and **4ab** in poor isolated yields (17% and 3%, respectively), probably due to the low solubilities of the starting materials and products in *o*-xylene. On the other hand, the amination of **3b**, which has a sterically-demanding alkyl group (*t*-Bu) on the benzofuranyl unit, resulted in D-A compounds **4ba**, **4bb**, **4bc**, and **4bd** in moderate to good yields (Table 2), probably due to the increased solubilities of the substrates and the products. Amination of **3b** with phenothiazine, acridone, and diphenylamine also successfully gave the corresponding products **4be**, **4bf**, and **4bg**, albeit in low yields. The versatility of this protocol starting from 2,6-dihalopyridine was demonstrated by preparing a variety of regio isomers of D-A compounds (i.e., **4ba**, **4ca**, **4da**, **4fa**, and **4ga**), which would allow for structure-properties relationship (SPR) studies. Furthermore, this method allows for the syntheses of D–A conjugated compounds whose electron-withdrawing ability is enhanced with a CF_3 group (**4ha**, **4hc**, **4hd**, **4hg**, and **4ic**).

Table 2. Synthesis of donor-substituted BBZFPys through Buchwald-Hartwig amination of **3**[a]

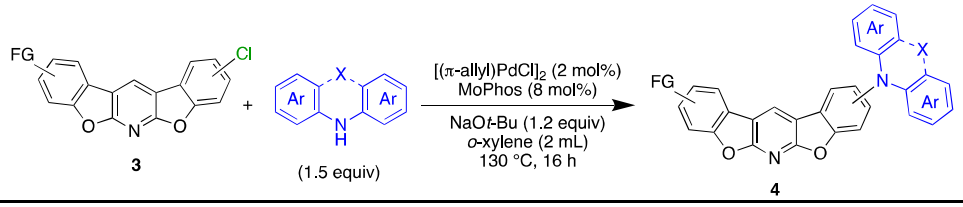

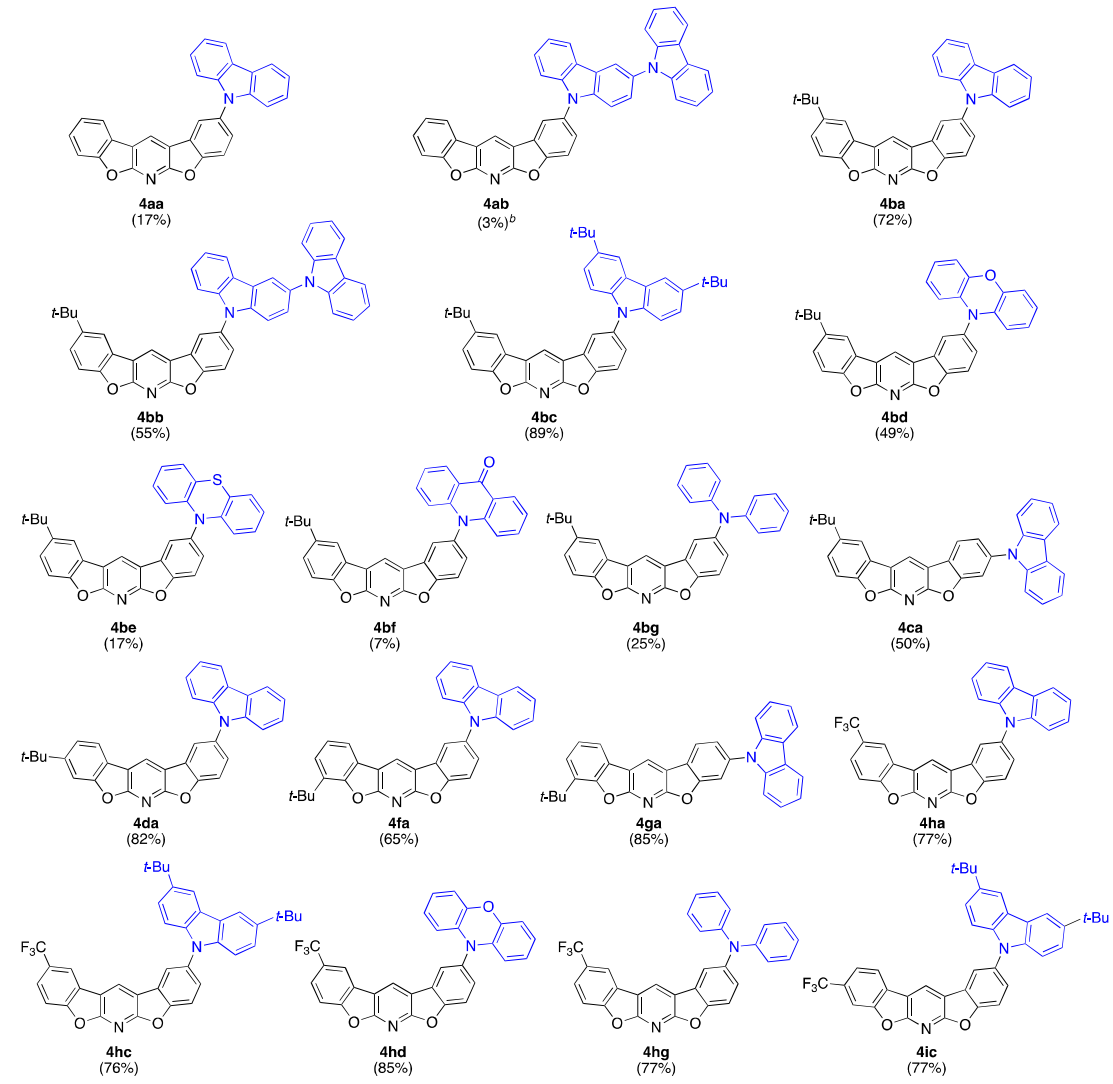

[a]Reaction conditions: **3** (0.50 mmol), [(π-allyl)PdCl]$_2$ (10 μmol, 2 mol%), MoPhos (40 μmol, 8 mol%), and NaO*t*-Bu (0.60 mmol, 1.2 equiv) in *o*-xylene (2.0 mL) in a 10 mL Schlenk tube at 130 °C for 16 h under N_2 atmosphere. [b] 3.0 mL of *o*-xylene was used as the solvent.

Steady-State Photophysical Properties

To explore the possibilities of the D-A-type BBZFPys as emissive materials for optoelectronic devices, the steady-state photophysical properties in diluted solutions and solid states were investigated. Figure 2 illustrates representative UV-vis absorption and steady-state photoluminescence (PL) spectra of **4aa**, **4bc**, **4bd**, **4hc**, and **4ic** in solutions (Figure 2a, c, e, g, and i) and in the solid state (Figure 2b, d, f, h, and j) (for other compounds, see the Figure S6–S8), and the properties of all the D-A compounds are summarized in Table 3 and 4. Typically, in $CHCl_3$ solutions, almost all the compounds exhibited an absorption at around 290 nm and structured absorptions ranging from 330 nm to 380 nm (Figure 2a, c, e, g, and i), which are very similar to that of non-substituted BBZFPy.[6] Upon the irradiation of UV light, all the compounds are emissive in solution in violet-to-green region, with the PLQYs ranging from 0.01 to 0.71 (Table 3). Steady-state photoluminescence (PL) spectra of the $CHCl_3$/EtOH (1:4 *v/v*) solution of **4aa** recorded at room temperature showed a broad Gaussian-type shape peaked at 448 nm (Figure 2a, green line). When compared with non-substituted BBZFPy,[6] the Stokes shift is much larger (6547 cm^{-1} for **4aa**, 1041 cm^{-1} for BBZFPy), which is typical to the emissions from the singlet charge-transfer excited state (^{1}CT) of D-A type conjugated compounds. In fact, distinct positive-solvatochromism of the emissions were observed with a D-A compound **4hc**, which has an electron-withdrawing group (CF_3) on the BBZFPy acceptor core (Figure S9, Table S12). In the cases of **4ab**, **4ba**, **4bb**, **4bc**, **4bg**, **4da**, **4fa**, **4hc**, along with the ^{1}CT emissions, the remnant emissions from the local excited state of the acceptor (^1LE_A) or the donor (^1LE_D) were observed (Figure 2c, g; Figure S6a, c, e; Figure S7a, e, g), which would reflect the slow electron transfer (EA) process within these molecules due to significantly twisted D-A geometries.[9g,f,10c] The population of the ^{1}LE and ^{1}CT emissions is inverted in the cases of phenoxazine- and phenothiazine-, and acridone-substituted BBZFPys (**4bd**, **4be**, and **4bf**, Figure 2e, Figure S6g, and Figure S6i, respectively), implying their perpendicularly twisted and rigid D-A geometries in solutions to suppress the ET process from the D to A units. This was supported by the PES scans of a series of D-A compounds **4aa**, **4bd**, **4bd**, **4bf**, and **4bg** (Figure S1–5): Compounds **4bd**, **4be**, and **4bf** have the potential minima where the D-A interplanar angles make a right angle, while **4aa** and **4bg** take less twisted angles (*ca.* 58° and 42 °, respectively) at the potential minima. All the phosphorescence (PH) spectra recorded at 77 K in the $CHCl_3$/EtOH (1:4 *v/v*) solutions looked alike, featured with vibronic structures (e.g., blue lines in Figure 2a, c, e, g, and i), and they are almost superimposed with the PH spectrum of non-substituted BBZFPy.[6] This strongly suggests that the nature of the excited triplet states of the D-A compounds are almost correlated with that of the local excited triple state of BBZFPy (^3LE_A).[6] Owing to the stabilized ^{1}CT states and the dominant contribution of the ^3LE_A in their triplet excited states with a high energy

level (at around 2.88 eV), the singlet-triplet energy splitting ($\Delta E_{1CT\text{-}3LE}$) in solution are narrower than that of BBZFPy (0.70 eV) in all cases, ranging from 0.01 to 0.56 (Table 3). Overall, quantum yields are very low except for **4bf** and **4ca**. Taken together with the facts that these D-A compounds also have small $\Delta E_{1CT\text{-}3LE}$, it is speculated that either efficient intersystem crossing (ISC) process followed by non-radiative decays based on the molecular rotation and/or vibration or charge recombination leading to the "dark" state are the possible reasons for such low quantum yields.

In the solid states, several compounds that contain carbazoles as the donor (e.g., **4aa**, **4ba**, **4bc**, and **4da**) showed aggregation-induced enhanced emission (AIEE) properties,[14] implying that twisted geometries suppress intermolecular π-π interactions in the solid states. Judged from the similarity of the phosphorescence spectra between the solution and solid states, the triplet nature of D-A-type BBZFPys **4** can be correlated with the ^{3}LE states of the acceptor. Interesting features were observed with **4aa**, **4ba**, **4fa**, and **4ga**, where dual emissions were observed, one with structured PH (λ_{em} 450–700 nm) from the ^3LE_A as observed in solutions and the one overlapped with the PL from the ^{1}LE of the donor or acceptor (λ_{em} 350–450 nm).

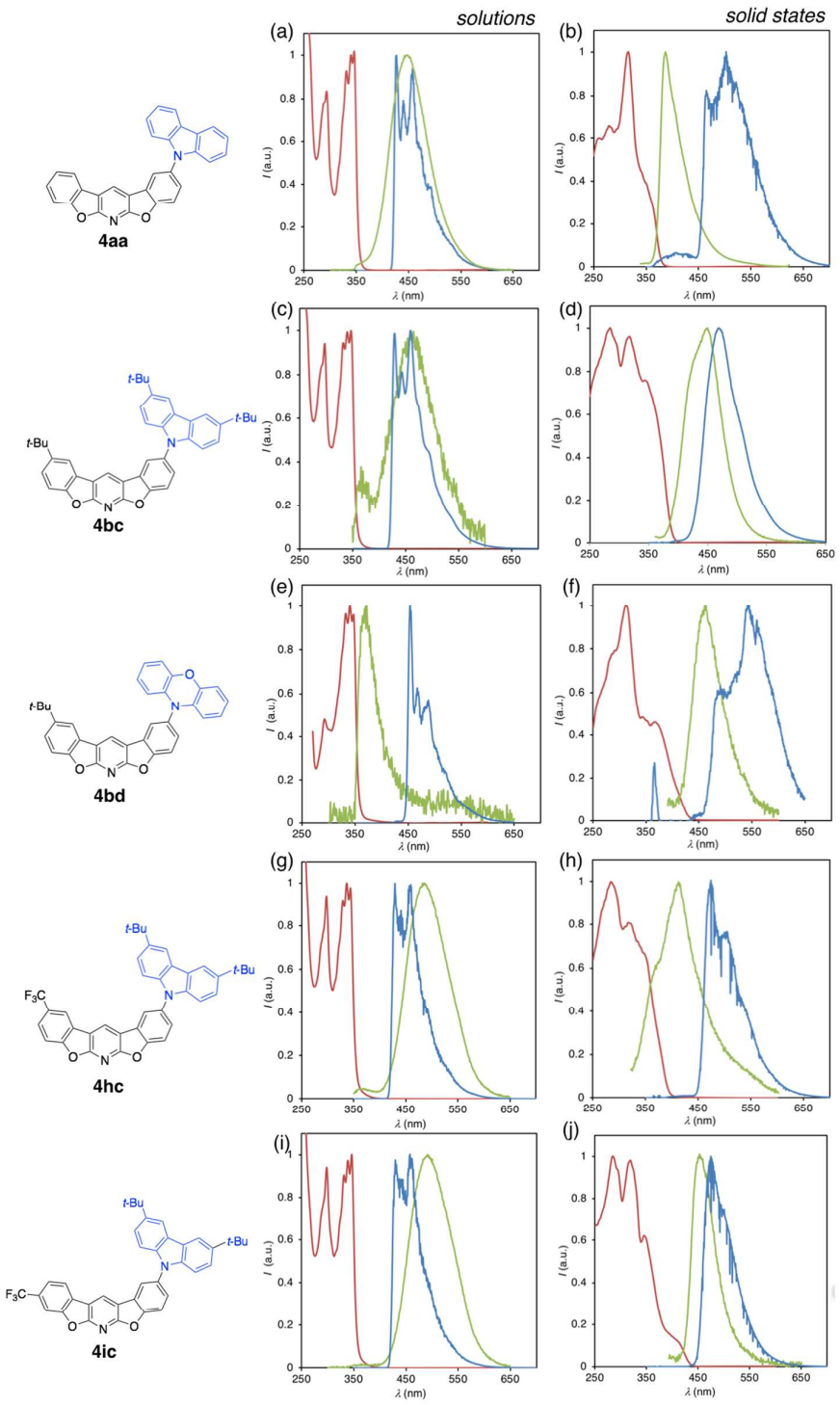

Figure 2. (a), (c), (e), (g), and (i) Normalized UV-vis absorption (red, 50 μM, $CHCl_3$), fluorescence (green, 50 μM, EtOH/$CHCl_3$ 4:1 *v/v* measured at room temperature), and phosphorescence (blue, 10 μM, EtOH/$CHCl_3$ 4:1 *v/v* measured at 77K) of diluted solutions of **4aa**, **4bc**, **4bd**, **4hc**, and **4ic**. (b), (d), (f), (h), and (j) Normalized absorption (red), fluorescence (green, measured at room temperature), and phosphorescence (blue, measured at 77K) of **4aa**, **4bc**, **4bd**, **4hc**, and **4ic** in the solid state.

Table 3. Selected photophysical data of diluted solutions of D-A compounds

Compd	λ_{abs} (nm)[a]	$^{PL}\lambda_{em}$ (nm)[a,b]	Φ_{PL} (%)[a,c]	$^{PH}\lambda_{em}$ (nm)[d]	E_{1CT} (eV)[e]	E_{3LE} (eV)[f]	$\Delta E_{1CT\text{-}3LE}$ (eV)
4aa	294, 330, 340, 346	448	0.074	426, 440, 459	3.24	2.96	0.28
4ab	294, 354	489	0.027	426, 439, 457	3.10	2.97	0.13
4ba	294, 335, 342, 348	446	0.076	429, 443, 459	3.30	2.95	0.35
4bb	334, 343, 348	446	0.150	429, 443, 461	3.30	2.95	0.35
4bc	298, 337, 342, 346	444	0.044	428, 444, 462	3.28	2.95	0.33
4bd	295, 334, 341, 347	491	0.057	454, 469, 490	–[g]	2.81	-
4be	295, 337, 342, 348	371, 524	0.016	495, 532	-[g]	2.68	-
4bf	375, 396	409, 431	0.391	476, 510	3.09	2.72	0.37
4bg	263, 319, 339, 342	379, 465	0.083	470	3.01	2.85	0.16
4ca	332, 340, 347	396	0.714	450, 480	3.36	2.84	0.52
4da	294, 336, 344, 350	417	0.075	432, 446, 464	3.30	2.89	0.41
4fa	293, 333, 342, 348	419	0.072	425, 439, 456	3.27	2.97	0.30
4ga	294, 355	397	0.704	449, 480	3.41	2.96	0.45
4ha	292, 330, 339, 342	438	0.074	426, 440, 456	3.23	3.00	0.23
4hc	297, 331, 338, 345	364, 460	0.058	428, 460	3.07	3.00	0.07
4hd	289, 330, 343, 344	489	0.055	455, 469, 489	2.81	2.82	0.02
4hg	328, 338, 345	487	0.099	477	2.87	2.86	0.01
4ic	298, 333, 340, 346	466	0.065	429, 461	3.05	2.98	0.07

[a] Measured at room temperature using $CHCl_3$ solutions ($c \sim 50$ μM). [b] $^{PL}\lambda_{em}$ indicates the lowest-energy wavelength of the maximum emission. [c] Absolute quantum yields were measured with a spectrometer equipped with an integrated sphere. [d] Measured at 77 K using EtOH/$CHCl_3$ = 4:1 ($c \sim 50$ μM). [e] Determined from the following equation: $E_{1CT} = 1240/\lambda_{onset,\ 1CT}$, where $\lambda_{onset,\ 1CT}$ indicates the onset wavelength (nm) of the CT emission observed at room temperature. [f] Determined from the following equation: $E_{3LE} = 1240/\lambda_{onset,\ 3LE}$, where $\lambda_{onset,\ 3LE}$ indicates the onset wavelength (nm) of the phosphorescence emission observed at 77 K. [g] Due to the absence of CT emission, E_{1CT} value was not estimated.

Table 4. Selected photophysical data of D-A compounds in solid states

Compd	λ_{abs} (nm)[a]	$^{PL}\lambda_{em}$ (nm)[a,b]	Φ_{PL} (%)[a,c]	$^{PH}\lambda_{em}$ (nm)[d]	E_{1CT} (eV)[e]	E_{3LE} (eV)[f]	$\Delta E_{1CT\text{-}3LE}$ (eV)
4aa	316	387	0.216	464, 504	3.37	2.74	0.63

4ab	-	388	0.040	-	3.82	-	-
4ba	286, 318, 345	410, 434	0.210	410, 438, 487, 503, 527, 548, 565, 597	3.16	2.64	0.52
4bb	281, 319, 343	416	0.126	483, 495	3.21	2.86	0.35
4bc	285, 318, 346	450	0.185	470	3.22	2.92	0.30
4bd	314, 348, 370	464	0.067	495, 544, 560	3.02	2.68	0.34
4be	320, 377	493	-	516, 556	2.88	2.48	0.40
4bf	318, 348, 376, 393	433, 458	0.097	–	3.02	-	-
4bg	284, 386	460	0.066	470	3.01	2.85	0.16
4ca	332, 340, 347	396	0.304	507, 524	3.01	2.64	0.37
4da	283, 318, 352	426	0.221	476, 512	3.26	2.81	0.45
4fa	281, 324	401	0.073	410, 468, 487, 520	3.37	2.85	0.52
4ga	286, 329	415	0.218	416, 477, 517	3.02	2.68	0.34
4ha	282, 320, 365	419	0.094	438, 476, 501	3.24	2.81	0.43
4hc	287, 322, 349	414	0.071	476, 506	-[g]	2.75	–
4hd	316, 364	383	0.061	551, 568	-[g]	2.44	–
4hg	287	456	0.132	532	2.99	2.58	0.41
4ic	286, 320, 349, 414	455	0.063	476	2.92	2.77	0.15

[a] Measured at room temperature. [b] PL λ_{em} indicates the lowest-energy wavelength of the maximum emission. [c] Absolute quantum yields were measured with a spectrometer equipped with an integrated sphere. [d] Measured at 77 K. [e] Determined from the following equation: $E_{1CT} = 1240/\lambda_{onset,\ 1CT}$, where $\lambda_{onset,\ 1CT}$ indicates the onset wavelength (nm) of the CT emission observed at room temperature. [f] Determined from the following equation: $E_{3LE} = 1240/\lambda_{onset,\ 3LE}$, where $\lambda_{onset,\ 3LE}$ indicates the onset wavelength (nm) of the phosphorescence emission observed at 77 K. [g] The CT and LE emissions seem to be overlapped, and the CT emission is too weak. Therefore, the ^{1}CT energies cannot be determined.

Time-Resolved Photophysical Analysis

To investigate the dynamic behavior of the photo-excited states of a promising D-A compound **4hc** that shows a small $\Delta E_{1CT\text{-}3LE}$, time-resolved luminescence spectroscopy of **4hc** was performed in both inert non-polar Zeonex®□ host (Figure 3a and b) and DPEPO host (Figure 4a and b), the latter of which was used to mimic the chemical environment within an OLED device. Also, to explore the effect of the CF_3 position of the BBZFPy core on photophysical properties, the

photophysics of **4ic**, which is a regioisomer of **4hc**, was also investigated (Figure 3c, d; Figure 4c, d). Both showed emissions within two distinct time regions. The first, decaying with a lifetime within the nanosecond time regime in all the materials, is attributed to prompt emission from the singlet excited state due to its temperature independence (Figure 3a, c; Figure 4a, c). The emission spectra acquired in both Zeonex® and DPEPO at the time delay (TD) of 3 ns showed a Gaussian-like peak (black and green lines in Figure 3b, d; Figure 4b, d) that decayed quite fast and then reappeared in almost the same place (blue lines in Figure 3b, d) or in the lower energy region (blue line in Figure 4d) over longer times. The first species can be attributed to the emission from the charge transfer (^{1}CT) singlet excited state. The energy onset of this CT emission follows the same trend as observed in solution (Figure 2): 3.38 eV for **4hc** and 3.32 eV for **4ic** in Zeonex®; 3.28 eV for **4hc** and 3.20 eV for **4ic** in DPEPO host.

At the longer delay times, in the microsecond/millisecond delay time regions, delayed emission (DE) was observed in Zeonex® (Figure 3a, c). Depending upon the experimental temperature, both the singlet state DE and triplet state emission were observed on similar millisecond timescales, and therefore the emission from each state is most easily elucidated upon spectral inspection at different temperatures (Figure 3a, c). At ambient temperature, the DE was observed with the same spectral shape and onset energy as the prompt CT spectra (Figure 3b, d). Therefore, it can be identified as delayed fluorescence (DF), but the emission is so weak, it would be difficult to distinguish between TADF and triplet-triplet annihilation (TTA)[15] process. With all the materials, the emission from the triplet state was observed at a low temperature (80 K), with this triplet energy being found at 3.00 eV (**4hc**) and 2.98 (**4ic**) in Zeonex® (Figure 3b, d) and 2.96 eV (**4hc**) and 2.96 (**4ic**) in DPEPO (Figure 4b, d). From the energetical point of view, ΔE_{ST} of the materials are estimated to be 0.38 eV (**4hc**) and 0.36 (**4ic**) in Zeonex® (Figure 3b, d), and 0.32 eV (**4hc**) and 0.24 eV (**4ic**) in DPEPO (Figure 4b, d). These moderate values suggested a moderate exchange energy, probably due to the moderate D-A twisted angles.

As for the compounds in Zeonex® host, we can conclude that there is some DF contribution, while in DPEPO host, their behavior is different. It seems that there is no DF emission at all. Moreover, the delayed emission disappeared for compound **4hc** at a higher temperature (Figure 4b). What is interesting, in the film composed of compound **4ic** with the DPEPO host, there was a weak room temperature phosphorescence (RTP), which might be a candidate for RTP materials for future organic electronic applicastions.[16]

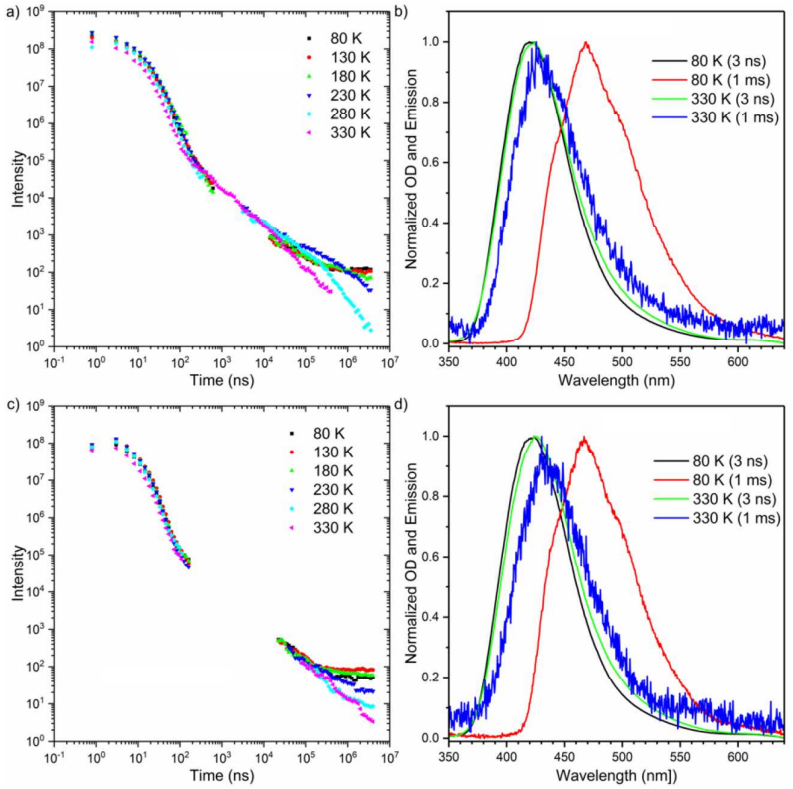

Figure 3. (a) Plot of 1% *w/w* **4hc** in Zeonex® emission intensity against delay time measured 80 K (black), 130 K (red), 180 K (green), 230 K (blue), 280 K (cyan), 330 K (pink). (b) Normalized intensity spectra of 1% *w/w* **4hc** in Zeonex® at both 330 K and 80 K. (c) Plot of 1% *w/w* **4ic** in Zeonex® emission intensity against delay time measured 80 K (black), 130 K (red), 180 K (green), 230 K (blue), 280 K (cyan), 330 K (pink). (d) Normalized intensity spectra of 1% *w/w* **4ic** in Zeonex® at both 330 K and 80 K.

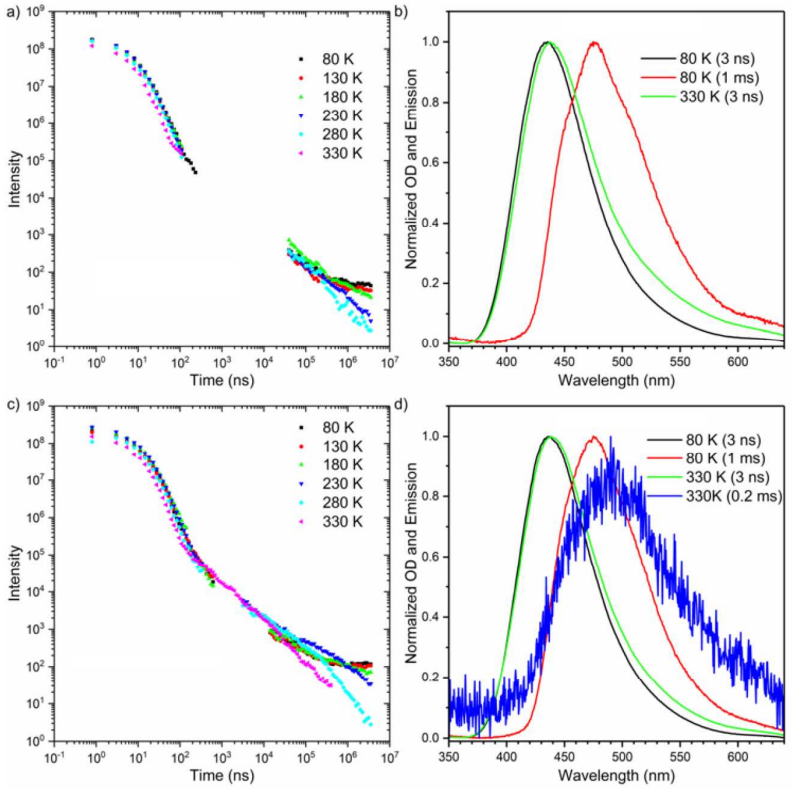

Figure 4. (a) Plot of 10% *w/w* **4hc** in DPEPO emission intensity against delay time measured 80 K (black), 130 K (red), 180 K (green), 230 K (blue), 280 K (cyan), 330 K (pink). (b) Normalized emission spectra of 10% *w/w* **4hc** in DPEPO at varying delay times at 330 K and 80 K. (c) Plot of 10% *w/w* **4ic** in DPEPO emission intensity against delay time measured 80 K (black), 130 K (red), 180 K (green), 230 K (blue), 280 K (cyan), 330 K (pink). (d) Normalized emission spectra of 10% *w/w* **4ic** in DPEPO at varying delay times at 330 K and 80 K.

OLED Applications

Before applying the compounds **4hc** and **4ic** as blue emitters in OLED devices, their thermal stabilities were investigated with thermogravimetric analyses (TGA). The degradation temperatures (defined at 5 wt% loss) T_d of **4hc** and **4ic** under air were found over 330 °C (Figure S10), which are high enough for the purification and deposition of OLED devices with vacuum thermal deposition method. As the final step of the analyses, the OLED devices were fabricated (Figure 5). The device structures of [ITO/NPB (50 nm)/CzSi (10 nm)/10% **4hc** (dev 1) or **4ic** (dev 3) in mCP (20 nm)/TPBi (50 nm)/LiF (1 nm)/Al (100 nm)] and [ITO/NPB (40 nm)/CzSi (10 nm)/10% **4hc** (dev 2) or **4ic** (dev 4) in DPEPO (20 nm)/DPEPO (10 nm)/TPBi (50 nm)/LiF (1 nm)/Al (100 nm)] were chosen for comparison (Figure 5). The inspection of the characteristics of the fabricated OLED revealed that the EL observed in all the devices are ascribed to the CT emissions from the compounds **4hc** and **4ic**. The overall efficiency is moderate (around 1%), which

should be caused by low delayed fluorescence contribution. The most efficient devices were the ones fabricated with DPEPO host, which resulted an efficiency around 1.5% external quantum efficiency (EQE) with the brightness up to 2000 cd/m^2 (Figure 5). The turn-on voltage was between 2 V (dev 2) and 3 V (dev 1), while the OLED characteristic showed the roll-off dependency, especially for device 4.

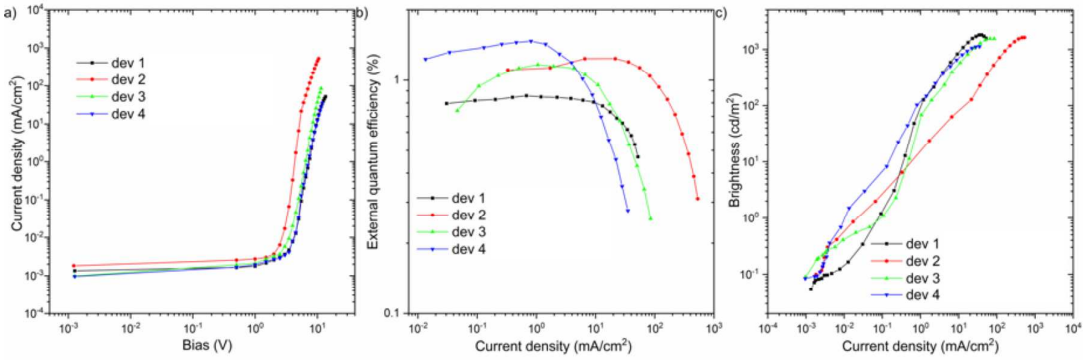

Figure 5. Device characteristic of dev 1–4.

Conclusion

In conclusion, we have established a highly atom- and step-economical synthetic procedures for diverse D-A-structured BBZFPys utilizing a Pd-catalyzed intramolecular double C–H/C–H oxidative coupling of chlorinated 2,6-diaryloxypyridines and the subsequent Buchwald-Hartwig amination. With this protocol, a series of regioisomers of D-A-type BBZFPys are selectively accessible. The steady-state photophysical investigation of the D-A compounds has showed that they are emissive in violet-to-green region, with ΔE_{ST} values being moderately narrow in solution and solid states. Time-resolved inspection has revealed the host-dependent involvement of delayed fluorescence from **4hc** and **4ic** in Zeonex® host, while the **4ic** in DPEPO shows RTP. Furthermore, these compounds have been demonstrated to be utilized as blue-emitters in OLED devices, with the EQE achieving 1.5 %.

Experimental Section

General Experimental Methods. Nuclear magnetic resonance spectra were measured operating at 400 MHz (^{1}H NMR), at 100 MHz (^{13}C NMR), and at 376 MHz (^{19}F NMR). ^{1}H NMR chemical shifts were reported in ppm relative to the resonance in TMS at δ 0.00. ^{13}C NMR chemical shifts were reported in ppm relative to the residual solvent signals of $CDCl_3$ at δ 77.16. High resolution mass spectra (HRMS) were recorded with APCI-TOF. Melting points were measured with Mettler Toledo MP90. GC analysis was carried out using a Shimadzu silicon OV-17 column (2.6 mm × 1.5

m). UV-vis spectra were acquired with Shimadzu UV-2500 PC and JASCO V-750 spectrometers. PL spectra and PLQY measurements were conducted with Shimadzu RF-5300PC Spectro Fluoro Photometer (fluorescence) and JASCO FP-8500 Spectro Fluoro Photometer (phosphorescence). The DFT calculations were performed by using the Gaussian 09 package.[17]

Materials. DMSO, NMP, and *o*-xylene were dried over CaH_2 and distilled under reduced pressure before use. All the other reagents were purchased from commercial sources and used as received without further purification.

General procedure for the preparation of 2-chloro-6-aryloxypyridines 1a–1d (*Conditions A* in Scheme 1): To a flask (50 mL) equipped with a magnetic stirring bar, 2,6-dichloropyridine (2.20 g, 15 mmol), phenol derivative (7.5 mmol), and K_2CO_3 (8.29 g, 60 mmol) were added, and the atmosphere inside the flask was replaced with N_2 gas. DMSO (20 mL) was added to the flask with a syringe, and the resulting solution was stirred at 160 °C for 24 h. After the reaction completed, AcOEt (20 mL) and water (20 mL) were added to the reaction mixture, and the organic layer was extracted with AcOEt for 3 times, dried with Na_2SO_4, and filtered through activated alumina. The filtrate was concentrated under reduced pressure to give oil residue, which was then dissolved in an eluent and purified by column chromatography on silica gel. Further purification was conducted with GPC.

2-Chloro-6-phenoxypyridine (1a) [CAS No. 23628-24-2]. Purified by column chromatography (eluent *n*-hex/AcOEt 20:1) on silica gel followed by GPC ($CHCl_3$). 2.01 g, 93%, white solid; m.p. 83.8–85.8 °C; ^{1}H NMR (400 MHz, $CDCl_3$) δ 6.73 (dd, *J* = 8.1, 0.6 Hz, 1H), 7.03 (dd, *J* = 7.6, 0.6 Hz, 1H), 7.12–7.15 (m, 2H), 7.22 (tt, *J* = 7.5, 1.1 Hz, 1H), 7.38–7.43 (m, 2H), 7.61 (dd, *J* = 8.0, 8.1 Hz, 1H); ^{13}C NMR (100 MHz, $CDCl_3$) δ 109.2, 118.6, 121.1, 125.2, 129.9, 141.5, 149.2, 153.7, 163.2; HRMS (APCI) *m/z* $(M+H)^+$ calcd for $C_{11}H_9ClNO$: 206.0367, found: 206.0367. All the spectroscopic data are in accordance with the literature.[18]

2-Chloro-6-(4-*tert*-butylphenoxy)pyridine (1b). Purified by column chromatography (eluent *n*-hex/AcOEt 10:1) on silica gel followed by GPC ($CHCl_3$). 2.59 g, 94%,white solid; m.p. 61.4–62.4 °C; ^{1}H NMR (400 MHz, $CDCl_3$) δ 1.34 (s, 9H), 6.71 (dd, *J* = 8.1, 0.5 Hz, 1H), 7.02 (dd, *J* = 7.6, 0.6 Hz, 1H), 7.07 (dd, *J* = 6.7, 2.1 Hz, 2H), 7.40 (dd, *J* = 6.7, 2.1 Hz, 2H), 7.59 (dd, *J* = 8.1, 8.1 Hz, 1H); ^{13}C NMR (100 MHz, $CDCl_3$): δ 31.6, 34.6, 109.0, 118.4, 120.4, 126.8, 141.4, 148.0, 149.2, 151.3, 163.5; HRMS (APCI) *m/z* $(M+H)^+$ calcd for $C_{15}H_{17}ClNO$: 262.0993, found: 262.1006.

2-Chloro-6-(3-*tert*-butylphenoxy)pyridine (1c). Prepared by following a general procedure using 20 mmol of 2,6-dichloropyridine, 14 mmol of 3-*tert*-butylphenol, 80 mmol of K_2CO_3, and 20 mL of DMSO. Purified by column chromatography (eluent *n*-hex/AcOEt 10:1) on silica gel followed by GPC ($CHCl_3$). 3.43 g, 88%, colorless oil; ^{1}H NMR (400 MHz, $CDCl_3$) δ 1.32 (s, 9H), 6.70 (d, *J* = 8.0 Hz, 1H), 6.95 (ddd, *J* = 7.9, 2.4, 1.0 Hz, 1H), 7.03 (d, *J* = 7.6 Hz, 1H), 7.17

(dd, J = 2.1, 2.1 Hz, 1H), 7.24 (ddd, J = 7.7, 1.6, 1.1 Hz, 1H), 7.32 (dd, J = 7.9, 7.9 Hz, 1H), 7.60 (dd, J = 7.9, 7.9 Hz, 1H); ^{13}C NMR (100 MHz, $CDCl_3$) δ 31.3, 34.8, 108.9, 117.8, 118.2, 118.4, 122.1, 129.3, 141.4, 149.1, 153.52, 153.56, 163.3; HRMS (APCI) *m/z* $(M+H)^+$ calcd for $C_{15}H_{17}ClNO$: 262.0993, found: 262.0992.

2-Chloro-6-(2-*tert*-butylphenoxy)pyridine (1d). Prepared by following a general procedure using 20 mmol of 2,6-dichloropyridine, 14 mmol of 3-*tert*-butylphenol, 80 mmol of K_2CO_3, and 20 mL of DMSO. Purified by column chromatography (eluent *n*-hex/AcOEt 10:1) on silica gel followed by GPC ($CHCl_3$). 3.37 g, 92%, white solid; m.p. 36.1–37.8 °C; ^{1}H NMR (400 MHz, $CDCl_3$) δ 1.37 (s, 9H), 6.66 (d, J = 8.1 Hz, 1H), 6.95 (dd, J = 7.8, 1.4 Hz, 1H), 7.03 (d, J = 7.6 Hz, 1H), 7.13–7.23 (m, 2H), 7.44 (dd, J = 7.7, 1.7 Hz, 1H), 7.59 (dd, J = 7.8, 7.8 Hz, 1H); ^{13}C NMR (100 MHz, $CDCl_3$) δ 30.3, 34.7, 109.3, 118.3, 122.5, 125.0, 127.2, 127.6, 141.4, 141.6, 149.4, 152.6, 163.5; HRMS (APCI) *m/z* $(M+H)^+$ calcd for $C_{15}H_{17}ClNO$: 262.0993, found: 262.0998.

General procedure for the preparation of 2-bromo-6-aryloxypyridines 1e and 1f (*Conditions B* in Scheme 1): These compounds were prepared by modifying a reported procedure.[11] To a flask (100 mL) equipped with a magnetic stirring bar, 2,6-dibromopyridine (6.39 g, 27 mmol), CuI (514.2 mg, 2.7 mmol, 10 mol%), picolinic acid (664.8 mg, 5.4 mmol, 20 mol%), and K_3PO_4 (11.46 g, 54 mmol) were added, and the atmosphere inside the flask was replaced with N_2 gas. Phenol derivative (15 mmol) was dissolved into DMSO (50 mL), which then was added to the flask with a syringe, and the resulting solution was stirred at 90 °C for 24 h. After the reaction completed, AcOEt (80 mL), water (80 mL), and ethylenediamine (10 mL) were added to the reaction mixture, and the organic layer was extracted with AcOEt for 3 times, dried with Na_2SO_4, and filtered through activated alumina. The filtrate was concentrated under reduced pressure to give oil residue, which was then dissolved in an eluent and purified by column chromatography on silica gel. Further purification was conducted with GPC.

2-Bromo-6-[4-(trifluoromethyl)phenoxy]pyridine (1e). Purified by column chromatography (eluent *n*-hex/AcOEt 5:1) on silica gel followed by GPC ($CHCl_3$). 2.41g, 51%, pale yellow oil; ^{1}H NMR (400 MHz, $CDCl_3$) δ 6.89 (dd, J = 8.1, 0.6 Hz, 1H), 7.24–7.27 (m, 3H), 7.58 (dd, J = 7.7, 7.7 Hz, 1H), 7.66 (dd, J = 8.9, 0.4 Hz, 2H); ^{13}C NMR (100 MHz, $CDCl_3$) δ 110.5, 121.0, 123.4, 124.1 (q, J = 272.0 Hz), 127.0 (q, J = 33 Hz), 127.1 (q, J = 3.7 Hz), 139.2, 141.6, 156.5, 162.0; ^{19}F NMR (376 MHz, $CDCl_3$) δ –61.99; HRMS (APCI) *m/z* $(M+H)^+$ calcd for $C_{12}H_8BrF_3NO$: 317.9736, found: 317.9735.

2-Bromo-6-[3-(trifluoromethyl)phenoxy]pyridine (1f). Purified by column chromatography (eluent *n*-hex/AcOEt 10:1) on silica gel followed by GPC ($CHCl_3$). 3.58 g, 75%, pale yellow oil; ^{1}H NMR (400 MHz, $CDCl_3$) δ 6.87 (d, J = 8.0 Hz, 1H), 7.23–7.26 (m, 1H), 7.35 (dd, J = 7.9, 1.7 Hz, 1H), 7.42 (s, br, 1H), 7.46–7.59 (m, 3H); ^{13}C NMR (100 MHz, $CDCl_3$) δ 110.2,

118.2 (q, J =3.7 Hz), 121.7 (q, J = 4.0 Hz), 123.2, 123.7 (q, J = 273.1 Hz), 124.4, 130.3, 1321.29 (q, J = 33.0 Hz), 139.27, 141.5, 153.9, 162.2; ^{19}F NMR (376 MHz, $CDCl_3$) δ –62.66; HRMS (APCI) m/z $(M+H)^+$ calcd for $C_{12}H_8BrF_3NO$: 317.9736, found: 317.9735.

General procedure for the preparation of 2a–2g (*Conditions C* in Scheme 1): To a flask equipped with a magnetic stirring bar, 2-halo-6-aryloxypyridine **1** (9.81 mmol), phenol derivative (11.7 mmol), and K_2CO_3 (4.06 g, 29.4 mmol) were added, and the atmosphere inside the flask was replaced with N_2 gas. DMSO (13 mL) was added to the flask with a syringe, and the resulting solution was stirred at 160 °C for 24 h. After the reaction completed, AcOEt and water were added to the reaction mixture, and the organic layer was extracted with AcOEt for 3 times, dried with Na_2SO_4, and filtered through activated alumina. The filtrate was concentrated under reduced pressure to give oil residue, which was then dissolved in $CHCl_3$ and purified by column chromatography on silica gel. Further purification was conducted with GPC.

2-(4-Chlorophenoxy)-6-phenoxypyridine (2a). Purified by column chromatography (eluent *n*-hex/AcOEt 10:1) on silica gel followed by GPC ($CHCl_3$). 2.62 g, 80%, pale yellow oil; ^{1}H NMR (400 MHz, $CDCl_3$) δ 6.52 (ddd, J = 8.0, 7.9, 0.5 Hz, 2H), 6.99–7.11 (m, 4H), 7.17 (tt, J = 7.4, 1.2 Hz, 1H), 7.23–7.28 (m, 2H), 7.30–7.35 (m, 2H), 7.64 (dd, J = 8.0, 8.0 Hz, 1H); ^{13}C NMR (100 MHz, $CDCl_3$) δ 104.4, 121.2, 121.3, 122.6, 122.7, 124.8, 129.4, 129.5, 142.3, 152.4, 153.8, 162.0, 162.5; HRMS (APCI) m/z $(M+H)^+$ calcd for $C_{17}H_{13}ClNO_2$: 298.0629, found: 298.0628.

2-(4-*tert*-Butylphenoxy)-6-(4-chlorophenoxy)pyridine (2b) [CAS No. 2085326-80-1]. Prepared by following a general procedure on a 6 mmol scale (**1b**). Purified by column chromatography (eluent *n*-hex/AcOEt 20:1) on silica gel followed by GPC ($CHCl_3$). 1.52 g, 72%, colorless oil; Spectroscopy data were in good agreement with those reported previously.[6] ^{1}H NMR (400 MHz, $CDCl_3$) δ 1.33 (s, 9H), 6.49 (dd, J = 8.0, 0.5 Hz, 1H), 6.51 (dd, J = 7.9, 0.5 Hz, 1H), 6.97 (d, J = 8.9 Hz, 2H), 7.02 (d, J = 8.9 Hz, 2H), 7.23 (d, J = 8.9 Hz, 2H), 7.31 (d, J = 8.9 Hz, 2H), 7.62 (dd, J = 7.9, 7.8 Hz, 1H); HRMS (APCI) m/z $(M+H)^+$ calcd for $C_{21}H_{21}NO_2Cl$: 354.1255, found: 354.1264. All the spectroscopic data are in accordance with the literature.[6]

2-(4-*tert*-Butylphenoxy)-6-(3-chlorophenoxy)pyridine (2c) [CAS No. 2085326-82-3]. Prepared by following a general procedure on a 11.5 mmol scale (**1b**). Purified by column chromatography (eluent *n*-hex/AcOEt 20:1) on silica gel followed by GPC ($CHCl_3$). 2.47 g, 61%, colorless oil; ^{1}H NMR (400 MHz, $CDCl_3$) δ 1.31 (s, 9H), 6.53 (dd, J = 7.5, 7.4 Hz, 2H), 6.97–7.02 (m, 3H), 7.08–7.12 (m, 2H), 7.21 (dd, J = 8.3, 8.1 Hz, 1H), 7.32–7.34 (m, 2H), 7.64 (dd, J = 8.2, 7.9 Hz, 1H); ^{13}C NMR (100 MHz, $CDCl_3$) δ 31.5, 34.5, 104.4, 104.6, 119.5, 120.7, 121.7, 124.7, 126.4, 130.1, 134.5, 142.3, 147.5, 151.3, 154.6, 161.82, 162.81; HRMS (APCI) m/z $(M+H)^+$ calcd for $C_{21}H_{21}ClNO_2$: 354.1255, found: 354.1245. All the spectroscopic data are in accordance with the literature.[6]

2-(3-*tert*-Butylphenoxy)-6-(4-chlorophenoxy)pyridine (2d). Prepared by following a general procedure on a 5.73 mmol scale (**1c**). Purified by column chromatography (eluent *n*-hex/AcOEt 10:1) on silica gel followed by GPC ($CHCl_3$). 1.45 g, 72%, colorless oil; ^{1}H NMR (400 MHz, $CDCl_3$) δ 1.27 (s, 9H), 6.48 (d, *J* = 7.8 Hz, 1H), 6.54 (d, *J* = 7.8 Hz, 1H), 6.88 (ddd, *J* = 7.8, 2.4, 1.1 Hz, 1H), 7.02–7.04 (m, 2H), 7.08 (dd, *J* = 2.1, 2.1 Hz, 1H), 7.18–7.27 (m, 4H), 7.63 (dd, *J* = 7.8, 7.8 Hz, 1H); ^{13}C NMR (100 MHz, $CDCl_3$) δ 31.3, 34.8, 104.2, 104.4, 118.3, 118.5, 121.8, 122.6, 129.1, 129.4, 129.6, 142.3, 152.4, 153.3, 153.7, 162.0, 162.8; HRMS (APCI) *m/z* $(M+H)^+$ calcd for $C_{21}H_{21}ClNO_2$: 354.1255, found: 354.1257.

2-(3-*tert*-Butylphenoxy)-6-(3-chlorophenoxy)pyridine (2e). Prepared by following a general procedure on a 5.73 mmol scale (**1c**). Purified by column chromatography (eluent *n*-hex/AcOEt 10:1) on silica gel followed by GPC ($CHCl_3$). 1.27 g, 63%, yellow oil; ^{1}H NMR (400 MHz, $CDCl_3$) δ 1.27 (s, 9H), 6.50 (dd, *J* = 8.0, 0.5 Hz, 1H), 6.56 (dd, *J* = 7.9, 0.5 Hz, 1H), 6.90 (ddd, *J* = 8.0, 2.3, 1.1 Hz, 1H), 6.99 (ddd, *J* = 8.2, 2.3, 1.0 Hz, 1H), 7.08–7.11 (m, 3H), 7.17–7.28 (m, 3H), 7.65 (dd, *J* = 7.9, 7.9 Hz, 1H); ^{13}C NMR (100 MHz, $CDCl_3$) δ 31.3, 34.8, 104.6, 104.7, 118.2, 118.4, 119.4, 121.6, 121.8, 124.6, 129.0, 130.1, 134.6, 142.3, 153.3, 153.7, 154.7, 161.7, 162.8; HRMS (APCI) *m/z* $(M+H)^+$ calcd for $C_{21}H_{21}ClNO_2$: 354.1255, found: 354.1237.

2-(2-*tert*-Butylphenoxy)-6-(4-chlorophenoxy)pyridine (2f). Prepared by following a general procedure on a 5.73 mmol scale (**1d**). Purified by column chromatography (eluent *n*-hex/AcOEt 10:1) on silica gel followed by GPC ($CHCl_3$). 1.65 g, 82%, colorless oil; ^{1}H NMR (400 MHz, $CDCl_3$) δ 1.33 (s, 9H), 6.48–6.51 (m, 2H), 6.89–6.92 (m, 1H), 7.00–7.04 (m, 2H), 7.08–7.15 (m, 2H), 7.21–7.25 (m, 2H), 7.36–7.39 (m, 1H), 7.63 (dd, *J* = 7.9, 7.9 Hz, 1H); ^{13}C NMR (100 MHz, $CDCl_3$) δ 30.4, 34.7, 104.1, 105.0, 122.5, 123.2, 124.7, 126.9, 127.3, 129.4, 129.6, 141.5, 1421.2, 152.6, 152.7, 162.1, 162.9; HRMS (APCI) *m/z* $(M+H)^+$ calcd for $C_{21}H_{21}ClNO_2$: 354.1255, found: 354.1255.

2-(2-*tert*-Butylphenoxy)-6-(3-chlorophenoxy)pyridine (2g). Prepared by following a general procedure on a 5.73 mmol scale (**1d**). Purified by column chromatography (eluent *n*-hex/AcOEt 10:1) on silica gel followed by GPC ($CHCl_3$). 1.66 g, 82%, colorless oil; ^{1}H NMR (400 MHz, $CDCl_3$) δ 1.33 (s, 9H), 6.53 (dd, *J* = 7.9, 7.9 Hz, 2H), 6.92 (dd, *J* = 7.8, 1.6 Hz, 1H), 6.96 (ddd, *J* = 8.2, 2.1, 1.0 Hz, 1H), 7.06–7.16 (m, 4H), 7.17–7.22 (m, 1H), 7.37 (dd, *J* = 7.8, 1.9 Hz, 1H), 7.65 (dd, *J* = 7.9, 7.9 Hz, 1H); ^{13}C NMR (100 MHz, $CDCl_3$) δ 30.4, 34.7, 104.4, 105.4, 119.2, 121.5, 123.1, 124.6, 124.7, 126.9, 127.3, 130.1, 134.5, 141.5, 142.3, 152.7, 154.8, 161.8, 162.9; HRMS (APCI) *m/z* $(M+H)^+$ calcd for $C_{21}H_{21}ClNO_2$: 354.1255, found: 354.1236.

General procedure for the preparation of 2h and 2i (*Conditions D* in Scheme 1): These compounds were prepared by modifying a reported procedure.[6] To a flask (20 mL) equipped with a magnetic stirring bar, 2-brom-6-aryloxypyridine **1e** or **1f** (5.00 mmol), phenol derivative (7.00

mmol), CuI (95.2 mg, 0.50 mmol, 10 mol%), and Cs_2CO_3 (2.44 g, 7.5 mmol) were added, and the atmosphere inside the flask was replaced with N_2 gas. NMP (10 mL) was added to the flask with a syringe, and the resulting solution was stirred at 160 °C for 24 h. After the reaction completed, AcOEt and water were added to the reaction mixture, and the organic layer was extracted with AcOEt for 3 times, dried with Na_2SO_4, and filtered through activated alumina. The filtrate was concentrated under reduced pressure to give oil residue, which was then dissolved in $CHCl_3$ and purified by column chromatography on silica gel. Further purification was conducted with GPC.

2-(4-Chlorophenoxy)-6-(4-(trifluoromethyl)phenoxy)pyridine (2h). Purified by column chromatography (eluent *n*-hex/AcOEt 10:1) on silica gel followed by GPC ($CHCl_3$). 1.65g, 90%, pale yellow oil; ^{1}H NMR (400 MHz, $CDCl_3$) δ 6.58 (dd, *J* = 8.0, 0.5 Hz, 1H), 6.62 (dd, *J* = 7.9, 0.5 Hz, 1H), 6.96–7.00 (m, 2H), 7.15 (d, *J* = 8.3 Hz, 2H), 7.22–7.26 (m, 2H), 7.56 (d, *J* = 8.4 Hz, 2H), 7.70 (dd, *J* = 8.0, 8.0 Hz, 1H); ^{13}C NMR (100 MHz, $CDCl_3$) δ 105.1, 121.4, 122.8, 124.2 (q, *J* = 270.7 Hz), 126.76 (q, *J* = 32.7 Hz), 126.78 (q, *J* = 3.7 Hz), 129.5, 130.1, 142.7, 152.2, 156.4, 161.4, 162.1; ^{19}F NMR (376 MHz, $CDCl_3$) δ –62.01; HRMS (APCI) *m/z* $(M+H)^+$ calcd for $C_{18}H_{12}ClF_3NO_2$: 366.0503, found: 366.0507.

2-(4-Chlorophenoxy)-6-(3-(trifluoromethyl)phenoxy)pyridine (2i). Purified by column chromatography (eluent *n*-hex/AcOEt 10:1) on silica gel followed by GPC ($CHCl_3$). 1.65 g, 90%, pale yellow oil; ^{1}H NMR (400 MHz, $CDCl_3$) δ 6.60 (dd, *J* = 8.0, 0.6 Hz, 1H), 6.61 (dd, *J* = 7.9, 0.5 Hz, 1H), 6.94–6.98 (m, 2H), 7.19–7.24 (m, 3H), 7.30–7.31 (m, 1H), 7.37–7.41 (m, 2H), 7.70 (dd, *J* = 8.0, 8.0 Hz, 1H); ^{13}C NMR (100 MHz, $CDCl_3$) δ 104.9, 105.1, 118.4 (q, *J* = 3.4 Hz), 121.4 (q, *J* =3.7 Hz), 122.7, 123.8 (q, *J* = 272.7 Hz), 124.8, 129.4, 130.00, 130.01, 131.9 (q, *J* = 33 Hz), 142.7, 152.2, 154.0, 161.6, 162.0; ^{19}F NMR (376 MHz, $CDCl_3$) δ –62.63; HRMS (APCI) *m/z* $(M+H)^+$ calcd for $C_{18}H_{12}ClF_3NO_2$: 366.0503, found: 366.0503.

General procedure for oxidative C–H/C–H coupling of 2: The reaction was conducted with a slightly modified procedure from those previously reported by our group.[6] To a Schlenk tube (10 mL) equipped with a magnetic stirring bar, 2,6-diaryloxypyridine **2** (0.40 mmol), $Pd(TFA)_2$ (13.2 mg, 0.04 mmol, 10 mol%), AgOAc (267.0 mg, 1.60 mmol), and PivOH (4.0 mL) were added under air, and the flask was capped with a septum. The mixture was stirred at 160 °C for 16 h. After the reaction completed, CH_2Cl_2 (5 mL) was added to the reaction mixture, and the resulting suspension was filtered through a Celite pad with an eluent of CH_2Cl_2 to remove the residue of silver. The filtrate was concentrated under reduced pressure to give. The solid was washed with hexane and methanol and collected and dried with suction filtration to give doubly cyclized product **3**. Any further purifications were not conducted, and the product **3** was used for the successive amination step.

2-Chlorobis(benzofuro)[2,3-*b*:3',2'-*e*]pyridine (3a). The title compound was prepared

under slightly modified conditions from a general procedure using $Pd(TFA)_2$ (26.4 mg, 0.08 mmol, 20 mol%), AgOAc (400.5 mg, 2.40 mmol), and **3a** was extracted with a Soxhlet extractor ($CHCl_3$, 4.5 h) and purified by washing with hexane followed by drying with suction filter. 125.8 gm, 80%, white solid; m.p. >300 °C; ^{1}H NMR (400 MHz, $CDCl_3$) δ 7.43–7.50 (m, 2H), 7.52–7.57 (m, 1H), 7.61 (dd, *J* = 8.7, 0.4 Hz, 1H), 7.69 (ddd, *J* = 8.3, 0.8, 0.8 Hz, 1H), 8.00 (dd, *J* = 2.1, 0.4 Hz, 1H), 8.03 (ddd, *J* = 7.6, 1.3, 0.6 Hz, 1H), 8.77 (s, 1H); ^{13}C NMR (100 MHz, $CDCl_3$) δ 109.0, 112.4, 112.5, 113.4, 120.6, 120.8, 122.9, 123.9, 124.3, 124.6, 127.71, 127.99, 129.3, 130.1, 137.4, 139.0, 154.9; HRMS (APCI) *m/z* $(M+H)^+$ calcd for $C_{17}H_9ClNO_2$: 294.0316, found: 294.0319.

2-(*tert*-Butyl)-10-chlorobis(benzofuro)[2,3-*b*:3',2'-*e*]pyridine (3b) [CAS No. 2085326-57-2]. 92.7 mg, 75%, white solid; m.p. 202.0–204.0 °C; ^{1}H NMR (400 MHz, $CDCl_3$) δ 1.46 (s, 9H), 7.37 (dd, *J* = 8.7, 2.2 Hz, 1H), 7.47 (d, *J* = 8.6 Hz, 1H), 7.49 (d, *J* = 8.7 Hz, 1H), 7.53 (dd, *J* = 8.6, 2.1 Hz, 1H), 7.97 (d, *J* = 2.1 Hz, 1H), 8.03 (d, *J* = 2.1 Hz, 1H), 8.63 (s, 1H); HRMS (APCI) *m/z* $(M+H)^+$ calcd for $C_{21}H_{17}NO_2Cl$: 350.0942, found: 350.0934. All the spectroscopic data are in accordance with the literature.[6]

2-(*tert*-Butyl)-9-chlorobis(benzofuro)[2,3-*b*:3',2'-*e*]pyridine (3c) [CAS No. 2085326-59-4]. Prepared by following a general procedure using 1.6 mmol of **2c**, $Pd(TFA)_2$ (0.16 mmol), AgOAc (6.4 mmol), and PivOH (16 mL) in a 50 mL Schlenk tube. 314.6 mg, 56%, white solid; m.p. 269.6–271.6 °C; ^{1}H NMR (400 MHz, $CDCl_3$) δ 1.45 (s, 9H), 7.42 (dd, *J* = 8.3, 1.8 Hz, 1H), 7.59–7.60 (m, 2H), 7.69 (d, *J* =1.8 Hz, 1H), 7.92 (d, *J* = 8.3 Hz, 1H), 8.02–8.03 (m, 1H), 8.79 (s, 1H); ^{13}C NMR (100 MHz, $CDCl_3$) δ 31.9, 35.1, 111.7, 112.5, 113.0, 114.3, 117.1, 121.2, 121.7, 122.1, 122.4, 124.3, 125.6, 133.1, 134.4, 147.1, 153.0, 154.8, 162.0; HRMS (APCI) *m/z* $(M+H)^+$ calcd for $C_{21}H_{17}ClNO_2$: 350.0942, found: 350.0947. All the spectroscopic data are in accordance with the literature.[6]

9-(*tert*-Butyl)-2-chlorobis(benzofuro)[2,3-*b*:3',2'-*e*]pyridine (3d). Prepared by following a general procedure using 1.6 mmol of **2d**, $Pd(TFA)_2$ (0.16 mmol), AgOAc (6.4 mmol), and PivOH (16 mL) in a 50 mL Schlenk tube. 110.9 mg, 19%,white solid; m.p. 249.6 °C (decomp.); ^{1}H NMR (400 MHz, $CDCl_3$) δ 1.43 (s, 9H), 7.45–7.51 (m, 2H), 7.59 (d, *J* = 8.7 Hz, 1H), 7.70 (s, 1H), 7.93 (d, *J* = 8.2 Hz, 1H), 7.97 (d, *J* = 1.7 Hz, 1H), 8.71 (s, 1H); ^{13}C NMR (100 MHz, $CDCl_3$) δ 31.7, 35.5, 109.2, 112.3, 113.9, 114.1, 119.8, 120.2, 120.55, 120.56, 121.5, 122.46, 122.47, 124.4, 127.5, 129.2, 152.4, 152.9, 155.3; HRMS (APCI) *m/z* $(M+H)^+$ calcd for $C_{21}H_{17}ClNO_2$: 350.0942, found: 350.0942.

3-(*tert*-Butyl)-9-chlorobis(benzofuro)[2,3-*b*:3',2'-*e*]pyridine (3e). Prepared by following a general procedure using 1.6 mmol of **2e**, $Pd(TFA)_2$ (0.16 mmol), AgOAc (6.4 mmol), and PivOH (16 mL) in a 50 mL Schlenk tube. 38.0 mg, 7%, white solid; m.p. 233.7–235.7 °C; ^{1}H NMR (400 MHz, $CDCl_3$) δ 1.44 (s, 9H), 7.41 (dd, *J* = 8.3, 1.8 Hz, 1H), 7.50 (dd, *J* = 8.3, 1.7 Hz, 1H), 7.70 (ddd, *J* = 4.2, 1.7, 0.4 Hz, 2H), 7.92 (ddd, *J* = 8.3, 4.5, 0.5 Hz, 2H), 8.73 (s, 1H); ^{13}C NMR (100 MHz,

$CDCl_3$) δ 31.7, 35.5, 108.0, 109.2, 112.5, 113.0, 114.1, 114.8, 118.3, 119.9, 120.2, 121.2, 121.4, 122.2, 124.3, 133.0, 135.9, 152.3, 155.3; HRMS (APCI) *m/z* $(M+H)^+$ calcd for $C_{21}H_{17}ClNO_2$: 350.0942, found: 350.0933.

8-(*tert*-Butyl)-2-chlorobis(benzofuro)[2,3-*b*:3',2'-*e*]pyridine (3f). Prepared by following a general procedure using 1.6 mmol of **2f**, $Pd(TFA)_2$ (0.16 mmol), AgOAc (6.4 mmol), and PivOH (16 mL) in a 50 mL Schlenk tube. 353.6 mg, 63%, white solid; m.p. 179.8–181.5 °C; ^{1}H NMR (400 MHz, $CDCl_3$) δ 1.60 (s, 9H), 7.36–7.40 (m, 1H), 7.45–7.49 (m, 2H), 7.61 (d, *J* = 8.8 Hz, 1H), 7.89 (d, *J* = 7.0 Hz, 1H), 7.99 (d, *J* = 2.2 Hz, 1H), 8.75 (s, 1H); ^{13}C NMR (100 MHz, $CDCl_3$) δ 29.9, 34.6, 112.1, 113.2, 133.7, 118.4, 120.4, 122.4, 122.7, 123.7, 124.2, 124.7, 127.4, 129.1, 135.8, 152.8, 153.0, 161.4, 161.7; HRMS (APCI) *m/z* $(M+H)^+$ calcd for $C_{21}H_{17}ClNO_2$: 350.0942, found: 350.0940.

8-(*tert*-Butyl)-3-chlorobis(benzofuro)[2,3-*b*:3',2'-*e*]pyridine (3g). Prepared by following a general procedure using 1.6 mmol of **2g**, $Pd(TFA)_2$ (0.16 mmol), AgOAc (6.4 mmol), and PivOH (16 mL) in a 50 mL Schlenk tube. 380.0 mg, 68%,white solid; m.p. 212.2–213.2 °C; ^{1}H NMR (400 MHz, $CDCl_3$) δ 1.60 (s, 9H), 7.36–7.47 (m, 3H), 7.70 (d, *J* = 1.6 Hz, 1H), 7.88 (dd, *J* = 7.6, 1.3 Hz, 1H), 7.93 (d, *J* = 8.3 Hz, 1H), 8.76 (s, 1H); ^{13}C NMR (100 MHz, $CDCl_3$) δ 29.9, 34.7, 112.5, 113.0, 113.8, 118.5, 121.2, 121.6, 122.3, 122.9, 123.7, 124.3, 124.8, 133.1, 135.9, 153.1, 154.8, 161.2, 161.7; HRMS (APCI) *m/z* $(M+H)^+$ calcd for $C_{21}H_{17}ClNO_2$: 350.0942, found: 350.0933.

2-Chloro-10-(trifluoromethyl)bis(benzofuro)[2,3-*b*:3',2'-*e*]pyridine (3h). Prepared by following a general procedure using 1.6 mmol of **2h**, $Pd(TFA)_2$ (0.16 mmol), AgOAc (6.4 mmol), and PivOH (16 mL) in a 50 mL Schlenk tube. 399.4 mg, 69%, white solid; m.p. 257.9–259.9 °C; ^{1}H NMR (400 MHz, $CDCl_3$) δ 7.50 (dd, *J* = 8.7, 2.0 Hz, 1H), 7.61 (d, *J* = 8.7 Hz, 1H), 7.76–7.82 (m, 2H), 7.99 (d, *J* = 2.0 Hz, 1H), 8.31 (s, 1H), 8.81 (s, 1H); ^{13}C NMR (100 MHz, $CDCl_3$) δ 112.8, 112.9, 113.3, 113.5, 118.4 (q, *J* = 4.0 Hz), 120.7, 123.0, 123.3, 123.8, 124.3 (q, *J* = 273.1 Hz), 125.0 (q, *J* = 3.7 Hz), 126.6 (q, *J* = 33.0 Hz), 128.2, 129.6, 153.1, 156.2, 162.31, 162.38; ^{19}F NMR (376 MHz, $CDCl_3$) δ –61.11; HRMS (APCI) *m/z* $(M+H)^+$ calcd for $C_{18}H_8ClF_3NO_2$: 362.0190, found: 362.0206.

2-Chloro-9-(trifluoromethyl)bis(benzofuro)[2,3-*b*:3',2'-*e*]pyridine (3i). Prepared by following a general procedure using 1.6 mmol of **2i**, $Pd(TFA)_2$ (0.16 mmol), AgOAc (6.4 mmol), and PivOH (16 mL) in a 50 mL Schlenk tube. 265.9 mg, 46%, white solid; m.p. 267.8–269.8 °C; ^{1}H NMR (400 MHz, $CDCl_3$) δ 7.50 (dd, *J* = 8.7, 2.1 Hz, 1H), 7.61 (d, *J* = 8.7 Hz, 1H), 7.72 (d, *J* = 8.1 Hz, 1H), 7.94 (s, 1H), 7.99 (d, *J* = 2.2 Hz, 1H), 8.12 (d, *J* = 8.1 Hz, 1H), 8.81 (s, 1H); ^{13}C NMR (100 MHz, $CDCl_3$) δ 110.0 (q, *J* = 4.0 Hz), 112.7, 113.4, 113.6, 120.8, 120.9 (q, *J* = 3.7 Hz), 121.2, 123.7, 123.9, 124.1 (q, *J* = 272.0 Hz), 125.8, 128.2, 129.6, 130.0 (q, *J* = 33.0 Hz), 153.2, 154.0, 162.5, 162.6; ^{19}F NMR (376 MHz, $CDCl_3$) δ –61.57; HRMS (APCI) *m/z* $(M+H)^+$ calcd for $C_{18}H_8ClF_3NO_2$: 362.0190, found: 362.0203.

General Procedure for Pd-Catalyzed Buchwald-Hartwig Amination of Chlorinated

BBZFPys: According to the literature,[13] the Buchwald-Hartwig amination of chlorinated BBZFPys were conducted by the following procedure: To the Schlenk tube (10 mL), chlorinated BBZFPy (e.g., **3d**, 175 mg, 0.50 mmol), [(π-allyl)PdCl]$_2$ (3.6 mg, 10 μmol, 2.0 mol%), MoPhos (14.0 mg, 40 μmol, 8.0 mol%), NaO*t*-Bu (57.6 mg, 0.6 mmol, 1.2 equiv) and *o*-xylene (2 mL) were added under the N_2 atmosphere. The resulting mixture was stirred at 130 °C for 16 h. After the reaction completed, AcOEt (20 mL) and water (20 mL) were added to the reaction mixture, and the organic layer was extracted with AcOEt for 3 times, dried with Na_2SO_4, and filtered through activated alumina. The filtrate was concentrated under reduced pressure to give solid. The resulting solid was dissolved in chloroform and purified by column chromatography on silica gel. Further purification was conducted with GPC ($CHCl_3$).

2-(9*H*-Carbazol-9-yl)bis(benzofuro)[2,3-*b*:3',2'-*e*]pyridine (4aa). Purified by column chromatography (eluent *n*-hex/AcOEt 10:1) on silica gel followed by GPC ($CHCl_3$). 35.9 mg, 17%, white solid; m.p. >300 °C; ^{1}H NMR (400 MHz, $CDCl_3$) δ 7.33 (ddd, *J* = 8.0, 6.1, 1.7 Hz, 2H), 7.41–7.47 (m, 5H), 7.55 (td, *J* = 8.2, 1.0 Hz, 1H), 7.70 (dd, *J* = 8.3, 2.2 Hz, 2H), 7.90 (d, *J* = 8.6 Hz, 1H), 8.01 (d, *J* = 7.6 Hz, 1H), 8.19–8.21 (m, 3H), 8.80 (s, 1H); ^{13}C NMR (100 MHz, $CDCl_3$) δ 109.7, 112.4, 113.0, 113.6, 113.9, 119.8, 120.2, 120.5, 120.8, 122.6, 123.0, 123.4, 123.9, 124.4, 126.2, 127.0, 127.9, 133.6, 141.5, 153.5, 154.9, 162.0, 162.2; HRMS (APCI) *m/z* $(M+H)^+$ calcd for $C_{29}H_{17}N_2O_2$: 425.1285, found: 425.1288.

2-(9*H*-[3,9'-Bicarbazol]-9-yl)bis(benzofuro)[2,3-*b*:3',2'-*e*]pyridine (4ab). Purified by column chromatography (eluent *n*-hex/AcOEt 10:1) on silica gel followed by GPC ($CHCl_3$). 9.4 mg, 3%, white solid; m.p. 197.2–198.2 °C; ^{1}H NMR (400 MHz, $CDCl_3$) δ 7.27–7.62 (m, 13H), 7.71 (d, *J* = 8.2 Hz, 1H), 7.79 (dd, *J* = 8.6, 2.3 Hz, 1H), 7.96 (d, *J* = 8.6 Hz, 1H), 8.02 (d, *J* = 7.0 Hz, 1H), 8.16–8.21 (m, 3H), 8.29 (d, *J* = 2.0 Hz, 1H), 8.34 (d, *J* = 1.2 Hz, 1H), 8.85 (s, 1H); ^{13}C NMR (100 MHz, $CDCl_3$) δ 109.9, 110.1, 110.8, 112.4, 112.9, 113.8, 114.0, 119.7, 119.8, 120.4, 120.86, 120.89, 122.6, 123.0, 123.1, 123.2, 123.9, 124.5, 124.6, 125.8, 126.0, 126.9, 128.0, 130.2, 133.3, 140.6, 141.6, 142.0, 142.2, 153.73, 153.78, 154.9, 162.1, 162.2; HRMS (APCI) *m/z* $(M+H)^+$ calcd for $C_{41}H_{24}N_3O_2$: 590.1863, found: 590.1863.

2-(*tert*-Butyl)-10-(9*H*-carbazol-9-yl)bis(benzofuro)[2,3-*b*:3',2'-*e*]pyridine (4ba). Purified by column chromatography (eluent *n*-hex/AcOEt 10:1) on silica gel followed by GPC ($CHCl_3$). 173.5 mg, 72%, white solid; m.p. 190.5–192.5 °C; ^{1}H NMR (400 MHz, $CDCl_3$) δ 1.44 (s, 9H), 7.33 (ddd, *J* = 8.0, 5.8, 2.1 Hz, 2H), 7.14–7.45 (m, 4H), 7.60–7.62 (m, 2H), 7.70 (dd, *J* = 8.7, 2.2 Hz, 1H), 7.90 (d, *J* = 8.7 Hz, 1H), 8.02 (s, 1H), 8.19–8.21 (m, 3H), 8.83 (s, 1H); ^{13}C NMR (100 MHz, $CDCl_3$) δ 31.9, 35.1, 107.3, 109.7, 111.7, 112.8, 113.6, 114.3, 117.2, 119.6, 120.2, 122.2, 122.8, 123.4, 124.5, 125.7, 126.2, 126.8, 133.6, 141.5, 147.5, 153.1, 153.5, 162.0, 162.3; HRMS (APCI) *m/z* $(M+H)^+$ calcd for $C_{33}H_{25}N_2O_2$: 481.1911, found: 481.1908.

2-(9*H*-[3,9'-Bicarbazol]-9-yl)-10-(*tert*-butyl)bis(benzofuro)[2,3-*b*:3',2'-*e*]pyridine (4bb). Purified by column chromatography (eluent *n*-hex/AcOEt 10:1) on silica gel followed by GPC ($CHCl_3$). 175.7 mg, 55%, white solid; m.p. 257.2–258.9 °C; ^{1}H NMR (400 MHz, $CDCl_3$) δ 1.46 (s, 9H), 7.30–7.39 (m, 3H), 7.44 (d, *J* = 3.6 Hz, 4H), 7.50–7.52 (m, 2H), 7.57–7.64 (m, 4H), 7.77 (dd, *J* = 8.6, 2.1 Hz, 1H), 7.93 (d, *J* = 8.6 Hz, 1H), 8.03 (s, 1H), 8.16–8.21 (m, 3H), 8.28 (d, *J* = 1.8 Hz, 1H), 8.34 (d, *J* = 1.5 Hz, 1H), 8.86 (s, 1H); ^{13}C NMR (100 MHz, $CDCl_3$) δ 31.9, 35.1, 109.9, 110.1, 110.8, 111.7, 112.6, 113.8, 114.4, 117.2, 119.6, 119.72, 119.78, 120.4, 120.6, 120.8, 122.1, 122.8, 123.0, 123.2, 124.5, 124.6, 125.77, 125.79, 126.0, 126.7, 126.9, 130.1, 131.0, 133.2, 140.5, 141.9, 142.1, 147.2, 153.1, 153.6, 162.0, 162.4; HRMS (APCI) *m/z* $(M+H)^+$ calcd for $C_{45}H_{32}N_3O_2$: 646.2489, found: 646.2492.

2-(*tert*-Butyl)-10-(3,6-di-*tert*-butyl-9*H*-carbazol-9-yl)bis(benzofuro)[2,3-*b*:3',2'-*e*]pyridine (4bc). Purified by column chromatography (eluent *n*-hex/AcOEt 10:1) on silica gel followed by GPC ($CHCl_3$). 265.7 mg, 89%, white solid; m.p. 210.2–212.2 °C; ^{1}H NMR (400 MHz, $CDCl_3$) δ 1.44 (s, 9H), 1.49 (s, 18H), 7.36 (dd, *J* = 8.6, 0.5 Hz, 2H), 7.49 (dd, *J* = 8.6, 2.0 Hz, 2H), 7.60–7.60 (m, 2H), 7.68 (dd, *J* = 8.7, 2.0 Hz, 1H), 7.86 (d, *J* = 8.6 Hz, 1H), 8.01 (dd, *J* = 1.7, 0.7 Hz, 1H), 8.17–8.19 (m, 3H), 8.81 (s, 1H); ^{13}C NMR (100 MHz, $CDCl_3$) δ 31.9, 32.1, 34.9, 35.1, 109.1, 111.6, 112.8, 113.4, 114.2, 116.4, 117.2, 119.2, 122.2, 122.7, 123.5, 123.9, 124.3, 125.6, 126.5, 134.1, 139.9, 143.1, 147.16 153.0, 153.2, 162.0, 162.3; HRMS (APCI) *m/z* $(M+H)^+$ calcd for $C_{41}H_{41}N_2O_2$: 593.3163, found: 593.3166.

2-(*tert*-Butyl)-10-(10*H*-phenoxazin-10-yl)bis(benzofuro)[2,3-*b*:3',2'-*e*]pyridine (4bd). Purified by column chromatography (eluent *n*-hex/AcOEt 20:1) on silica gel followed by GPC ($CHCl_3$). 121.1 mg, 49%, white solid; m.p. 163.1–165.2 °C; ^{1}H NMR (400 MHz, $CDCl_3$): 1.45 (s, 9H), 5.96 (dd, *J* = 8.0, 1.5 Hz, 2H), 6.60 (ddd, *J* = 7.4, 7.4, 1.6 Hz, 2H), 6.68 (ddd, *J* = 7.4, 7.4, 1.6 Hz, 2H), 6.74 (dd, *J* = 7.8, 1.6 Hz, 2H), 7.49 (dd, *J* = 8.6, 2.1 Hz, 1H), 7.60–7.61 (m, 2H), 7.89 (d, *J* = 8.6 Hz, 1H), 8.01–8.02 (m, 2H), 8.79 (s, 1H); ^{13}C NMR (100 MHz, $CDCl_3$) δ 31.9, 35.1, 111.7, 112.7, 113.4, 114.4, 114.9, 115.6, 117.2, 121.6, 122.1, 122.8, 123.3, 123.4, 125.6, 125.7, 130.1, 134.7, 143.8, 144.0, 147.2, 153.1, 153.9, 161.9, 162.3; HRMS (APCI) *m/z* $(M+H)^+$ calcd for $C_{33}H_{25}N_2O_3$: 497.1860, found: 497.1851.

2-(*tert*-Butyl)-10-(10*H*-phenothiazin-10-yl)bis(benzofuro)[2,3-*b*:3',2'-*e*]pyridine (4be). Purified by column chromatography (eluent *n*-hex/AcOEt 20:1) on silica gel followed by GPC ($CHCl_3$). 67.0 mg, 17%, green solid; m.p. >300 °C; ^{1}H NMR (400 MHz, $CDCl_3$) δ 1.45 (s, 9H), 6.23–6.25 (m, 2H), 6.83–6.87 (m, 4H), 7.05–7.07 (m, 2H), 7.55 (dd, *J* = 8.6, 2.1 Hz, 1H), 7.60–7.61 (m, 2H), 7.90 (d, *J* = 8.6 Hz, 1H), 8.01–8.07 (m, 2H), 8.79 (s, 1H); ^{13}C NMR (100 MHz, $CDCl_3$) δ 31.3, 35.1, 111.6, 112.7, 114.3, 114.4, 116.0, 117.2, 120.1, 122.1, 122.7, 122.8, 123.5, 125.3, 125.7, 126.9, 127.0, 130.5, 136.5, 144.6, 147.1, 153.0, 153.8, 161.9, 162.2; HRMS (APCI) *m/z* $(M+H)^+$

calcd for $C_{33}H_{25}N_2O_2S$: 513.1631, found: 513.1630.

10-(10-(*tert*-Butyl)bis(benzofuro)[2,3-*b*:3',2'-*e*]pyridin-2-yl)acridin-9(10*H*)-one (4bf). Purified by column chromatography (eluent *n*-hex/AcOEt 10:1) on silica gel followed by GPC ($CHCl_3$). 18.5 mg, 7%, brown solid; m.p. >300 °C; ^{1}H NMR (400 MHz, $CDCl_3$) δ 1.43 (s, 9H), 6.82 (d, *J* = 8.6 Hz, 2H), 7.30–7.34 (m, 2H), 7.50–7.54 (m, 3H), 6.60–7.64 (m, 2H), 7.99–8.04 (m, 3H), 8.64 (dd, *J* = 8.1, 1.5 Hz, 2H), 8.81 (s, 1H); ^{13}C NMR (100 MHz, $CDCl_3$) δ 31.9, 35.1, 111.7, 112.3, 114.7, 114.9, 116.9, 117.2, 121.9, 122.0, 122.1, 122.5, 123.0, 125.6, 125.9, 127.6, 129.0, 133.5, 134.7, 143.6, 147.3, 153.1, 154.5, 162.0, 162.5, 178.3; HRMS (APCI) *m/z* $(M+H)^+$ calcd for $C_{34}H_{25}N_2O_3$: 509.1860, found: 509.1860.

10-(*tert*-Butyl)-*N,N*-diphenylbis(benzofuro)[2,3-b:3',2'-e]pyridin-2-amine (4bg). Purified by column chromatography (eluent *n*-hex/AcOEt 10:1) on silica gel followed by GPC ($CHCl_3$). 60.6 mg, 25%, brown solid; m.p. 211.8–212.5 °C; ^{1}H NMR (400 MHz, CD_2Cl_2) δ 1.42 (s, 9H), 7.03 (tt, *J* = 7.3, 1.1 Hz, 2H), 7.10–7.13 (m, 4H), 7.26–7.31 (m, 5H), 7.57–7.59 (m, 3H), 7.78 (d, *J* = 2.3 Hz, 1H), 8.00 (s, 1H), 8.71 (s, 1H); ^{13}C NMR (100 MHz, $CDCl_3$) δ 31.9, 35.0, 111.6, 113.0, 113.2, 113.8, 117.0, 117.1, 122.3, 122.6, 122.7, 123.7, 123.9, 125.3, 125.4, 129.4, 144.3, 146.9, 148.3, 151.0, 152.9, 162.01, 162.04; HRMS (APCI) *m/z* $(M+H)^+$ calcd for $C_{33}H_{27}N_2O_2$: 483.2067, found: 483.2047.

2-(*tert*-Butyl)-9-(9*H*-carbazol-9-yl)bis(benzofuro)[2,3-*b*:3',2'-*e*]pyridine (4ca). Purified by column chromatography (eluent *n*-hex/AcOEt 10:1) on silica gel followed by GPC ($CHCl_3$). 120.7 mg, 50%, white solid; m.p. 190.5–192.5 °C; ^{1}H NMR (400 MHz, $CDCl_3$) 1.48 (s, 9H), 7.33 (dd, *J* = 7.5, 7.5 Hz, 2H), 7.45 (dd, *J* = 7.6, 7.2 Hz, 2H), 7.51 (d, *J* = 8.1 Hz, 2H), 7.62–7.67 (m, 3H), 7.91 (d, *J* = 1.5 Hz, 1H), 8.07 (s, 1H), 8.17–8.22 (m, 3H), 8.90 (s, 1H); ^{13}C NMR (100 MHz, $CDCl_3$) δ 31.9, 35.1, 109.8, 111.2, 111.7, 112.7, 114.3, 117.2, 120.4, 120.5, 121.5, 122.1, 122.2, 122.5, 122.7, 123.6, 125.6, 126.2, 137.0, 140.9, 147.1, 153.0, 155.2, 161.9, 162.0; HRMS (APCI) *m/z* $(M+H)^+$ calcd for $C_{33}H_{25}N_2O_2$: 481.1911, found: 481.1917.

9-(*tert*-Butyl)-2-(9*H*-carbazol-9-yl)bis(benzofuro)[2,3-*b*:3',2'-*e*]pyridine (4da). Purified by column chromatography (eluent *n*-hex/AcOEt 10:1) on silica gel followed by GPC ($CHCl_3$). 197.3 mg, 82%, white solid; m.p. >300 °C; ^{1}H NMR (400 MHz, $CDCl_3$): δ 1.44 (s, 9H), 7.31–7.35 (m, 2H), 7.40–7.50 (m, 5H), 7.68 (dd, *J* = 8.6, 2.0 Hz, 1H), 7.72 (s, 1H), 7.87–7.92 (m, 2H), 8.17–8.20 (m, 3H), 8.74 (s, 1H); ^{13}C NMR (100 MHz, $CDCl_3$) δ 31.6, 35.5, 109.1, 109.7, 112.7, 113.4, 114.0, 119.6, 119.8, 120.1, 120.2, 120.5, 121.4, 122.5, 123.4, 124.4, 126.1, 126.7, 133.4, 141.4, 152.3, 153.4, 155.3, 161.7, 162.1; HRMS (APCI) *m/z* $(M+H)^+$ calcd for $C_{33}H_{25}N_2O_2$: 481.1911, found: 481.1912.

8-(*tert*-Butyl)-2-(9*H*-carbazol-9-yl)bis(benzofuro)[2,3-*b*:3',2'-*e*]pyridine (4fa). Purified by column chromatography (eluent *n*-hex/AcOEt 10:1) on silica gel followed by GPC ($CHCl_3$).

156.8 mg, 65%, white solid; m.p. 284.5–285.8 °C; ^{1}H NMR (400 MHz, $CDCl_3$) δ 1.63 (s, 9H), 7.31–7.36 (m, 2H), 7.38 (d, *J* = 7.7 Hz, 1H), 7.41–7.48 (m, 5H), 7.69 (dd, *J* = 8.6, 2.1 Hz, 1H), 7.87 (dd, *J* = 7.6, 1.3 Hz, 1H), 7.91 (d, *J* = 8.6 Hz, 1H), 8.19–8.21 (m, 3H), 8.79 (s, 1H); ^{13}C NMR (100 MHz, $CDCl_3$) δ 29.9, 34.7, 109.7, 112.7, 113.6, 113.9, 118.5, 119.7, 120.2, 120.5, 122.8, 122.9, 123.4, 123.8, 124.4, 124.8, 126.2, 126.8, 133.5, 135.9, 141.5, 153.2, 153.5, 161.6, 162.1; HRMS (APCI) *m/z* $(M+H)^+$ calcd for $C_{33}H_{25}N_2O_2$: 481.1911, found: 481.1904.

8-(*tert*-Butyl)-3-(9*H*-carbazol-9-yl)bis(benzofuro)[2,3-*b*:3',2'-*e*]pyridine (4ga). Purified by column chromatography (eluent *n*-hex/AcOEt 10:1) on silica gel followed by GPC ($CHCl_3$). 203.5 mg, 85%, white solid; m.p. 244.4–247.1 °C; ^{1}H NMR (400 MHz, $CDCl_3$) δ 1.63 (s, 9H), 7.33 (t, *J* = 7.0 Hz, 2H), 7.39–7.53 (m, 6H), 7.67 (dd, *J* = 8.1, 1.8 Hz, 1H), 7.93 (dd, *J* = 7.7, 1.6 Hz, 2H), 8.18 (d, *J* = 7.7 Hz, 2H), 8.22 (d, *J* = 8.1 Hz, 1H), 8.87 (s, 1H); ^{13}C NMR (100 MHz, $CDCl_3$) δ 23.0, 34.7, 109.8, 111.2, 112.7, 113.9, 118.5, 120.4, 120.5, 121.6, 122.1, 122.4, 122.7, 123.0, 123.7, 123.8, 124.8, 126.2, 136.0, 137.0, 141.0, 153.2, 155.3, 161.3, 162.1; HRMS (APCI) *m/z* $(M+H)^+$ calcd for $C_{33}H_{25}N_2O_2$: 481.1911, found: 481.1908.

2-(9*H*-Carbazol-9-yl)-10-(trifluoromethyl)bis(benzofuro)[2,3-*b*:3',2'-*e*]pyridine (4ha). Purified by column chromatography (eluent *n*-hex/$CHCl_3$ 5:1) on silica gel followed by GPC ($CHCl_3$). 190.5 mg, 77%, white solid; m.p. 289.2–290.5 °C; ^{1}H NMR (400 MHz, $CDCl_3$) δ 7.32–7.35 (m, 2H), 7.40–7.46 (m, 4H), 7.72–7.74 (m, 1H), 7.78–7.83 (m, 2H), 7.89–7.92 (m, 1H), 8.18–8.22 (m, 3H), 8.30 (s, 1H), 8.86–8.87 (m, 1H); ^{13}C NMR (100 MHz, $CDCl_3$) δ 109.6, 112.7, 113.7, 118.4, 119.6, 119.8, 120.3, 120.5, 123.0, 123.5, 123.9, 124.9, 125.7, 120.2, 126.4, 126.7, 127.2, 127.4, 133.9, 141.4, 153.5, 156.2, 162.2, 162.5 (*Note: some signals were observed as broad and overlapped peaks, probably due to the presence of rotamers. Thus, it is difficult to identify the signals that are coupled with ^{19}F nuclei); ^{19}F NMR (376 MHz, $CDCl_3$) δ –61.13; HRMS (APCI) *m/z* $(M+H)^+$ calcd for $C_{30}H_{16}F_3N_2O_2$: 493.1158, found: 493.1157.

2-(3,6-Di-*tert*-butyl-9*H*-carbazol-9-yl)-10-(trifluoromethyl)bis(benzofuro)[2,3-*b*:3',2'-*e*]pyridine (4hc). Purified by column chromatography (eluent *n*-hex/$CHCl_3$ 5:1) on silica gel followed by GPC ($CHCl_3$). 229.8 mg, 76%, white solid; m.p. >300°C; ^{1}H NMR (400 MHz, $CDCl_3$) δ 1.49 (s, 18H), 7.36 (d, *J* = 8.7 Hz, 2H), 7.50 (dd, *J* = 8.7, 1.9 Hz, 2H), 7.71 (dd, *J* = 8.7, 2.1 Hz, 1 H), 7.77–7.82 (m, 2H), 7.87 (d, *J* = 8.7 Hz, 1H), 8.19–20 (m, 3H), 8.29 (s, 1H), 8.85 (s, 1H); ^{13}C NMR (100 MHz, $CDCl_3$) δ 32.1, 34.9, 109.0, 112.85, 112.89, 113.6, 113.9, 116.5, 118.4 (q, *J* = 4.2 Hz), 119.5, 123.1, 123.4, 123.5, 123.9, 124.3 (q, *J* = 270.5 Hz) 124.9 (q, *J* = 3.7 Hz), 125.7, 126.6 (q, *J* = 32.3 Hz), 127.2, 134.5, 139.8, 143.3, 153.4, 156.3, 162.3, 162.6; ^{19}F NMR (376 MHz, $CDCl_3$) δ –61.14; HRMS (APCI) *m/z* $(M+H)^+$ calcd for $C_{38}H_{32}F_3N_2O_2$: 605.2410, found: 605.2416.

2-(10*H*-phenoxazin-10-yl)-10-(trifluoromethyl)bis(benzofuro)[2,3-*b*:3',2'-*e*]pyridine (4hd). Purified by column chromatography (eluent *n*-hex/$CHCl_3$ 5:1) on silica gel followed by GPC

($CHCl_3$). 215.3 mg, 85%, yellow solid; m.p. 283.2–285.2 °C; ^{1}H NMR (400 MHz, $CDCl_3$) δ 5.95 (dd, *J* = 7.8, 1.4 Hz, 2H), 6.60 (td, *J* = 7.8, 1.5 Hz, 2H), 6.68 (td, *J* = 7.8, 1.4 Hz, 2H), 6.74 (dd, *J* = 7.8, 1.5 Hz, 2H), 7.53 (dd, *J* = 8.6, 2.1 Hz, 1H), 7.79–7.84 (m, 2H), 7.92 (d, *J* = 8.6 Hz, 1H), 8.05 (d, *J* = 2.1 Hz, 1H), 8.31 (s, 1H), 8.84 (s, 1H); ^{13}C NMR (100 MHz, $CDCl_3$) δ 112.8, 113.0, 113.4, 113.8, 115.1, 115.7, 118.5 (q, *J* = 4.2 Hz), 121.7, 123.0, 123.4, 123.6, 123.7, 124.3 (q, *J* = 271.6 Hz), 125.0 (q, *J* = 3.3 Hz), 125.1, 126.6 (q, *J* = 33.0 Hz), 130.8, 134.7, 135.1, 144.1, 154.1, 156.3, 162.3, 162.0; ^{19}F NMR (376 MHz, $CDCl_3$) δ –61.10; HRMS (APCI) *m/z* $(M+H)^+$ calcd for $C_{30}H_{16}F_3N_2O_3$: 509.1108, found: 509.1118.

***N,N*-Diphenyl-10-(trifluoromethyl)bisbenzofuro[2,3-b:3',2'-e]pyridin-2-amine (4hg).** Purified by column chromatography (eluent *n*-hex/AcOEt 10:1) on silica gel followed by GPC ($CHCl_3$). 191.0 mg, 77%, yellow solid; m.p. 261.9–263.3 °C; ^{1}H NMR (400 MHz, $CDCl_3$) δ 7.04 (t, *J* = 7.2 Hz, 2H), 7.12–7.14 (m, 4H), 7.26–7.30 (m, 4H), 7.33 (dd, *J* = 8.8, 2.2 Hz, 1H), 7.58 (d, *J* = 8.8 Hz, 1H), 7.75–7.80 (m, 3H), 8.23 (s, 1H), 8.72 (s, 1H); ^{13}C NMR (100 MHz, $CDCl_3$) δ 112.2, 112.6, 113.0, 114.2, 117.1, 118.2 (q, *J* = 3.9 Hz), 122.896, 122.898, 123.1, 123.4, 123.8, 124.3 (q, *J* = 271.4 Hz), 124.6 (q, *J* = 3.7 Hz), 125.8, 126.4 (q, *J* = 32.5 Hz), 129.5, 144.6, 148.2, 151.1, 156.0, 161.9, 162.5; ^{19}F NMR (376 MHz, $CDCl_3$) δ –61.14; HRMS (APCI) *m/z* $(M+H)^+$ calcd for $C_{30}H_{18}F_3N_2O_2$: 495.1315, found: 495.1295.

2-(3,6-Di-*tert*-butyl-9*H*-carbazol-9-yl)-9-(trifluoromethyl)bis(benzofuro)[2,3-*b*:3',2'-*e*] pyridine (4ic). Purified by column chromatography (eluent *n*-hex/$CHCl_3$ 3:1) on silica gel followed by GPC ($CHCl_3$). 232.8 mg, 77%, white solid; m.p. 291.8 °C (decomp.); ^{1}H NMR (400 MHz, $CDCl_3$): δ 1.49 (s, 18H), 7.35 (dd, *J* = 8.6, 0.5 Hz, 2H), 7.49 (dd, *J* = 8.6, 2.0 Hz, 2H), 7.71–7.74 (m, 2H), 7.90 (dd, *J* = 8.6, 0.5 Hz, 1H), 7.98 (s, 1H), 8.12 (d, *J* = 8.1 Hz, 1H), 8.19–8.20 (m, 3H), 8.86 (s, 1H); ^{13}C NMR (100 MHz, $CDCl_3$) δ 32.1, 34.9, 109.1, 109.8 (q, *J* = 4.0 Hz), 112.5, 113.6, 113.9, 116.5, 119.4, 120.8 (q, *J* = 3.7 Hz), 121.2, 123.5, 123.7, 123.8, 123.9, 124.3 (q, *J* = 272.5 Hz), 125.8, 127.1, 129.8 (q, *J* = 33.0 Hz), 134.5, 139.8, 143.3, 153.3, 154.0, 162.4, 162.7; ^{19}F NMR (376 MHz, $CDCl_3$) δ –61.54; HRMS (APCI) *m/z* $(M+H)^+$ calcd for $C_{38}H_{32}F_3N_2O_2$: 605.2410, found: 605.2405.

Photophysics. Photoluminescence spectra of thin films were recorded at room temperature with Edinburgh Instruments FLS980 fluorescence spectrometer with Xe-lamp as an excitation source and R-928 photomultiplier detector. Phosphorescence, prompt fluorescence (PF), and delayed fluorescence (DF) spectra and decays were recorded using nanosecond gated luminescence and lifetime measurements (from 400 ps to 1 s) using either third harmonics of a high energy pulsed Nd:YAG laser emitting at 355 nm (EKSPLA) or a N_2 laser emitting at 337 nm. Emission was focused onto a spectrograph and detected on a sensitive gated iCCD camera (Stanford Computer Optics) having a sub-nanosecond resolution. PF/DF time-resolved measurements were performed by exponentially increasing gate and integration times. Temperature-dependent experiments were

conducted using a continuous flow liquid nitrogen cryostat (Janis Research) under a nitrogen atmosphere.

Devices. OLEDs have been fabricated on pre-cleaned, patterned indium-tin-oxide (ITO) coated glass substrates with a sheet resistance of 20 Ω/sq and ITO thickness of 100 nm. All small molecules and cathode layers were thermally evaporated in Kurt J. Lesker Spectros II evaporation system under pressure of 10^{-6} mbar without breaking the vacuum. The sizes of pixels were 4 mm^2, 8 mm^2 and 16 mm^2.Organic semiconductors and aluminium were deposited at a rate of 1 $Å s^{-1}$, and the LiF layer was deposited at 0.1 $Å s^{-1}$. The characteristics of the devices were recorded using 6-inch integrating sphere (Labsphere) connected to a Source Meter Unit and Ocean Optics USB4000 spectrometer inside the glovebox. All materials were purchased from Sigma Aldrich or Lumtec and were purified by temperature-gradient sublimation in a vacuum.

Acknowledgements

This research was supported by JSPS KAKENHI Grant No. JP 17H06092 (Grant-in-Aid for Specially Promoted Research, to M.M.). Y.T. acknowledges the Grant-in-Aid for Scientific Research on Innovative Areas "π-System Figuration: Control of Electron and Structural Dynamism for Innovative Functions" (JSPS KAKENHI Grant No. JP17H05155). P.D. acknowledges the EU's Horizon 2020 for funding the ORZEL project under grant agreement No 691684. P.S. acknowledges the EU's Horizon 2020 for funding the HYPEROLED project under grant agreement No. 732013.

Supporting Information

Cartesian coordinates for the geometrical optimization studies, excitation energies, UV-Vis absorption and photoluminescence spectra, thermogravimetric analysis (TGA) profiles, and the copies of ^{1}H and ^{13}C NMR spectra of new compounds.

References

(1) (a) Krug, M.; Erlenkamp, G.; Sippl, W.; Schächtele, C.; Totzke, F.; Milgeroth, A. Discovery and Selectivity-Profiling of 4-Benzylamino 1-Aza-9-oxafluorene Derivatives as Lead Structures for IGF-1R Inhibitors. *Bioorg. Med. Chem. Lett.* **2010**, *20*, 6915–6919. (b) Krug, M.; Wichapong, K.; Erlenkamp, G.; Sippl, W.; Schächtele, C.; Totzke, F.; Hilgeroth, A. Discovery of 4-Benzylamino-Substituted α-Carbolines as a Novel Class of Receptor Tyrosine Kinase Inhibitors. *ChemMedChem* **2011**, *6*, 63–72.

(2) Lee, C. W.; Kim, J.-K.; Joo, S. H.; Lee, J. Y. High Quantum Efficiency Blue Phosphorescent Organic Light-Emitting Diodes Using 6-Position-Modified Benzofuro[2,3-*b*]pyridine Derivatives. *ACS Appl. Mater. Interfaces* **2013**, *5*, 2169–2173.

(3) (a) Ames, D. E.; Opalko, A. Palladium-Catalyzed Cyclisation of 2-Substituted Halogenoarenes by Dehydrohalogenation. *Tetrahedron* **1984**, *40*, 1919–1925. (b) Yue, W. S.; Li, J. J. A Concise Synthesis of All Four Possible Benzo[4,5]furopyridines via Palladium-Mediated Reactions. *Org. Lett.* **2002**, *4*, 2201–2203. (c) Liu, J.; Fitzgerald, A. E.; Mani, N. S. Facile Assembly of Fused Benzo[4,5]furo Heterocycles. *J. Org. Chem.* **2008**, *73*, 2951–2954. (d) Tobisu, M.; Kita, Y.; Ano, Y.; Chatani, N. Rhodium-Catalyzed Silylation and Intramolecular Arylation of Nitriles via Silicon-Assisted Cleavage of Carbon–Cyano Bonds. *J. Am. Chem. Soc.* **2008**, *130*, 15982–15989.

(4) (a) Yoshimoto, H.; Itatani, H. Palladium-Catalyzed Coupling Reaction of Aromatic Compounds. *Bull. Chem. Soc. Jpn.* **1973**, *46*, 2490–2492. (b) Shiotani, A.; Itatani, H. Dibenzofurans by Intramolecular Ring Closure Reactions. *Agnew. Chem., Int. Ed. Engl.* **1974**, *13*, 471–472. (c) Åkermark, B.; Eberson, L.; Jonsson, E.; Pettersson, E. Palladium-Promoted Cyclization of Diphenyl Ether, Diphenylamine, and Related Compounds. *J. Org. Chem.* **1975**, *40*, 1365–1367. (d) Hagelin, H.; Oslob, J. D.; Åkermark, B. Oxygen as Oxidant in Palladium-Catalyzed Inter- and Intramolecular Coupling Reactions. *Chem. Eur. J.* **1999**, *5*, 2413–2416. (e) Liégault, B.; Lee, D.; Huestis, M. P.; Stuart, D. R.; Fagnou, K. Intramolecular Pd(II)-Catalyzed Oxidative Biaryl Synthesis Under Air: Reaction Development and Scope. *J. Org. Chem.* **2008**, *73*, 5022–5028. (f) Oechsle, P.; Paradies, J. Ambidextrous Catalytic Access to Dithieno[3,2-*b*:2',3'-*d*]thiophene (DTT) Derivatives by Both Palladium-Catalyzed C–S and Oxidative Dehydro C–H Coupling. *Org. Lett.* **2014**, *16*, 4086–4089. (g) Saito, K.; Chikkade, P. K.; Kanai, M.; Kuninobu, Y. Palladium-Catalyzed Construction of Heteroatom-Containing π-Conjugated Systems by Intramolecular Oxidative C–H/C–H Coupling Reaction. *Chem. Eur. J.* **2015**, *21*, 8365–8368.

(5) (a) Kaida, H.; Satoh, T.; Hirano, K.; Miura, M. Synthesis of Thieno[3,2-*b*]benzofurans by Palladium-Catalyzed Intramolecular C–H/C–H Coupling. *Chem. Lett.* **2015**, *44*, 1125–1127. (b) Kaida, H.; Satoh, T.; Nishii, Y.; Hirano, K.; Miura, M. Synthesis of Benzobis- and Benzotrisbenzofurans by Palladium-Catalyzed Multiple Intramolecular C–H/C–H Coupling. *Chem. Lett.* **2016**, *45*, 1069–1071.

(6) Kaida, H.; Goya, T.; Nishii, Y.; Hirano, K.; Satoh, T.; Miura, M. Construction of Bisbenzofuro[2,3-*b*:3'2'-*e*]pyridines by Palladium-Catalyzed Double Intramolecular Oxidative C–H/C–H Coupling. *Org. Lett.* **2017**, *19*, 1236–1239.

(7) Miura, M.; Satoh, T.; Hirano, K. Development of Direct Aromatic Coupling Reactions by Transition-Metal Catalysis. *Bull. Chem. Soc. Jpn.* **2014**, *87*, 751–764.

(8) (a) Lin, Y.; Li, Y.; Zhan, X. Small Molecule Semiconductors for High-Efficiency Organic Photovoltaics. *Chem. Soc. Rev.* **2012**, *41*, 4245–4272. (b) Yang, Z.; Mao, Z.; Xi, Z.; Zhang, Y.; Liu, S.; Zhao, J.; Xu, J.; Chi, Z.; Aldred, M. P. Recent Advances in Organic Thermally Activated Delayed Fluorescence Materials. *Chem. Soc. Rev.* **2017**, *46*, 915–1016. (c) He, S.; Song, J.; Qu,

J.; Cheng, Z. Crucial Breakthrough of Second Near-Infrared Biological Window Fluorophores: Design and Synthesis toward Multimodal Imaging and Theranostics. *Chem. Soc. Rev.* **2018**, *47*, 4258–4278.

(9) (a) Uoyama H.; Goushi, K.; Shizu, K. Nomura, H.; Adachi, C. Highly Efficient Organic Light-Emitting Diodes from Delayed Fluorescence. *Nature* **2012**, *492*, 234–238. (b) Zhang, Q.; Li, J.; Shizu, K.; Huang, S.; Hirata, S.; Miyazaki, H.; Adachi, C. Design of Efficient Thermally Activated Delayed Fluorescence Materials for Pure Blue Organic Light Emitting Diodes. *J. Am. Chem. Soc.* **2012**, *134*, 14706–14709. (c) Dias, F. B.; Bourdakos, K. N.; Jankus, V.; Moss, K. C.; Kamtekar, K. T.; Bhalla, V.; Santos, J.; Bryce, M. R.; Monkman, A. P. Triplet Harvesting with 100% Efficiency by Way of Thermally Activated Delayed Fluorescence in Charge Transfer OLED Emitters. *Adv. Mater.* **2013**, *25*, 3707–3714. (d) Kawasumi, K.; Wu, T.; Zhu, T.; Chae, H. S.; Voorhis, T. V.; Baldo, M. A.; Swager, T. M. Thermally Activated Delayed Fluorescence Materials Based on Homoconjugation Effect of Donor–Acceptor Triptycenes. *J. Am. Chem. Soc.* **2015**, *137*, 11908–11911. (e) Cho, Y. J.; Jeon, S. K.; Chin, B. D.; Yu, E.; Lee, J. Y. The Design of Dual Emitting Cores for Green Thermally Activated Delayed Fluorescent Materials. *Angew. Chem., Int. Ed.* **2015**, *54*, 5201–5204. (f) Suzuki, K.; Kubo, S.; Shizu, K.; Fukushima, T.; Wakamiya, A.; Murata, Y.; Adachi, C.; Kaji, H. Triarylboron-Based Fluorescent Organic Light-Emitting Diodes with External Quantum Efficiencies Exceeding 20%. *Angew. Chem., Int. Ed.* **2015**, *54*, 15231–15235. (g) Data, P.; Pander, P. Okazaki, M.; Takeda, Y.; Minakata, S.; Monkman, A. P. Dibenzo[*a,j*]phenazine-Cored Donor-Accpetor-Donor Compounds as Green-to-Red/NIR Thermally Activated Delayed Fluorescence Organic Light Emitters. *Angew. Chem., Int. Ed.* **2016**, *55*, 5739–5744. (h) Okazaki, M.; Takeda, Y.; Data, P.; Pander, P.; Higginbotham, H.; Monkman, A. P.; Minakata, S. Thermally Activated Delayed Fluorescent Phenothiazine-dibenzo[*a,j*]phenazine-phenothiazine Trias Exhibiting Tricolor-Changing Mechanochromic Luminescence. *Chem. Sci.* **2017**, *8*, 2677–2686. and references therein.

(10) (a) Tao, Y.; Yuan, K.; Chen, T.; Xu, P.; Li, H.; Chen, R.; Zheng, C.; Zhang, L.; Huang, W. Thermally Activated Delayed Fluorescence Materials Towards the Breakthrough of Organoelectronics. *Adv. Mater.* **2014**, *26*, 7931–7958. (b) Dias, F. B.; Penfold, T. J.; Monkman, A. P. Photophysics of Thermally Activated Delayed Fluorescence Molecules. *Methods Appl. Fluoresc.* **2017**, *5*, 012001/1–25. (c) dos Santos, P. L.; Etherington, M. K.; Monkman, A. P. Chemical and Conformational Control of the Energy Gaps Involved in the Thermally Activated Delayed Fluorescence Mechanism. *J. Mater. Chem. C* **2018**, *6*, 4842–4853.

(11) Maiti, D.; Buchwald, S. L. Cu-Catalyzed Arylation of Phenols: Synthesis of Sterically Hindered and Heteroaryl Diaryl Ethers. *J. Org. Chem.* **2010**, *75*, 1791–1794.

(12) Sperotto, E.; de Vries, J. G.; van Klink, G. P. M.; van Koten, G. Ligand-Free Copper(I)

Catalyzed N- and O-Arylation of Aryl Halides. *Tetrahedron Lett.* **2007**, *48*, 7366–7370.

(13) Suzuki, K.; Hori, Y.; Kobayashi, T. A New Hybrid Phosphine Ligand for Palladium-Catalyzed Amination of Aryl Halides. *Adv. Synth. Catal.* **2008**, *350*, 652–656.

(14) Mei, J.; Leung, N. L. C.; Kwok, R. T. K.; Lam, J. W. Y.; Tang, B. Z. Aggregation-Induced Emission: Together We Shine, United We Soar! *Chem. Rev.* **2015**, *115*, 11718–11940.

(15) Sternlicht, H.; Nieman, G. C.; Robinson, G. W. Triplet–Triplet Annihilation and Delayed Fluorescence in Molecular Aggregates. *J. Chem. Phys.* **1963**, *38*, 1326–1335; **1963**, *39*, 1610–1611.

(16) (a) Mukherjee, S.; Thilagar, P. Recent Advances in Purely Organic Phosphorescent Materials. *Chem. Commun.* **2015**, *51*, 10988–11003. (b) Baroncini, M.; Bergamini, G.; Ceroni, P. Rigidification or Interaction-Induced Phosphorescence of Organic Materials. *Chem. Commun.* **2017**, *53*, 2081–2093. (c) Yuasa, H.; Kuno, S. *Bull. Chem. Soc. Jpn.* Intersystem Crossing Mechanisms in the Room Temperature Phosphorescence of Crystalline Organic Compounds. **2018**, *91*, 223–229. (d) Forni, A.; Lucenti, E.; Botta, C.; Cariati, E. Metal Free Room Temperature Phosphorescence from Molecular Self-Interactions in the Solid State. *J. Mater. Chem. C* **2018**, *6*, 4603–4626.

(17) Gaussian 09, Revision B.01, M. J. Frisch, G. W. Trucks, H. B. Schlegel, G. E. Scuseria, M. A. Robb, J. R. Cheeseman, G. Scalmani, V. Barone, B. Mennucci, G. A. Petersson, H. Nakatsuji, M. Caricato, X. Li, H. P. Hratchian, A. F. Izmaylov, J. Bloino, G. Zheng, J. L. Sonnenberg, M. Hada, M. Ehara, K. Toyota, R. Fukuda, J. Hasegawa, M. Ishida, T. Nakajima, Y. Honda, O. Kitao, H. Nakai, T. Vreven, J. A. Montgomery, Jr., J. E. Peralta, F. Ogliaro, M. Bearpark, J. J. Heyd, E. Brothers, K. N. Kudin, V. N. Staroverov, T. Keith, R. Kobayashi, J. Normand, K. Raghavachari, A. Rendell, J. C. Burant, S. S. Iyengar, J. Tomasi, M. Cossi, N. Rega, J. M. Millam, M. Klene, J. E. Knox, J. B. Cross, V. Bakken, C. Adamo, J. Jaramillo, R. Gomperts, R. E. Stratmann, O. Yazyev, A. J. Austin, R. Cammi, C. Pomelli, J. W. Ochterski, R. L. Martin, K. Morokuma, V. G. Zakrzewski, G. A. Voth, P. Salvador, J. J. Dannenberg, S. Dapprich, A. D. Daniels, O. Farkas, J. B. Foresman, J. V. Ortiz, J. Cioslowski, D. J. Fox, Gaussian, Inc., Wallingford CT, **2010**.

(18) Li, X.-H.; Ye, A.-H.; Liang, C.; Mo, D.-L. Substituted Effects of 2-Pyridones on Selective O-Arylation with Diaryliodonium Salts: Synthesis of 2-Aryloxypyridines under Transition-Metal-Free Conditions. *Synthesis* **2018**, *50*, 1699–1710.